UNIVERSIDADE DE LISBOA
FACULDADE DE CIÊNCIAS
DEPARTAMENTO DE BIOLOGIA VEGETAL

Mechanism of action and membrane selectivity of a novel antimicrobial peptide

Marcin Makowski

Mestrado em Microbiologia Aplicada

Dissertação orientada por:
Doutora Sónia Gonçalves e Prof. Ana Tenreiro

2016

Acknowledgments

Doing this work has been a fascinating journey. As in every adventure, I would like to say thank you to those people that have been along with me.

First things first: I want to thank Prof. Nuno Santos for accepting me in his group (for what I feel very honored), and to Sónia Gonçalves, for orienting this work and for encouraging me to do my best.

To Mário Felicio, who has got deeply involved in this work and has been extremely supportive; without his positive energy this experience would not have been the same.

To all the people from the Biomembranes group: I am very grateful for being so kind, supportive and helpful. Acknowledgements are also due to Prof. Octavio L. Franco, and for his group, for the scientific cooperation and for lending the peptide.

To the professors of the master's degree in applied microbiology.

Resumo

O número crescente de bactérias patogénicas resistentes aos antibióticos convencionais é atualmente uma das maiores preocupações, quer social como cientificamente. Com este cenário, a procura de alternativas terapêuticas tornou-se uma tarefa de enorme importância. Neste contexto, a investigação dedicada a péptidos antimicrobianos (AMP – *antimicrobial peptides*) tem aumentado, principalmente devido ao facto destas moléculas possuirem um grande espetro de ação contra uma variedade de agentes patogénicos (incluindo bactérias, vírus, fungos e parasitas). Mais especificamente, nos últimos anos, os esforços para sintetizar péptidos que possuam propriedades terapêuticas melhoradas em relação aos AMPs que se encontram na natureza têm aumentado. Com este objetivo em mente, estudos da relação entre atividade e propriedades físico-químicas dos AMP têm-se revelado de maior importância. Apesar de serem moléculas estruralmente muito variadas, algumas propriedades têm sido descritas como comuns, entre elas, a anfipaticidade e a carga global positiva. O principal mecanismo de ação até hoje descrito é a permeabilização seletiva das biomembranas dos organismos alvo, apresentando baixa ou nenhuma toxicidade para as células do organismo. Vários modelos têm sido propostos na tentativa de justificar o modo de ação dos AMPs na permeabilização de membranas, quer pela formação de poros que leva à destruição das membranas, quer mediante uma atividade de degradação direta, a qual se definiu como sendo "do tipo detergente". Quanto à seletividade membranar, as forças eletrostáticas têm uma grande contribuição. Enquanto as membranas de bactérias são ricas em lípidos aniónicos, o que promove a interação com os AMPs (altamente catiónicos), as membranas das células do hospedeiro possuem um folheto externo neutro (zwitteriónico), explicando-se assim a seletividade celular observada para vários AMPs. No entanto, vários estudos sugerem que componentes específicos das membranas bacterianas podem também desempenhar um papel importante na seletividade dos péptidos.

O *Ec*AMP1R2 é um péptido recentemente desenvolvido com base em modelos computacionais de desenho racional de AMPs, que toma em consideração as propriedades do mesmo e que poderão aumentar a actividade antimicrobiana. Especificamente, este AMP demonstrou uma elevada atividade antimicrobiana contra *E. coli*, uma bactéria Gram-negativa, responsável por diversas patologias infecciosas. É relevante referir que este péptido não apresenta atividade contra células humanas. *Ec*AMP1R2 tem uma carga global positiva (+5), numa sequência de 19 resíduos de aminoácidos. Em estudos preliminares observou-se

que adota preferencialmente uma estrutura secundária em α-hélice, aquando da presença de sistemas membranares hidrofóbicos, contrariamente ao apresentado em solução aquosa, onde não se observou uma estrutura definida (*random coiled*). Ao longo deste trabalho, estudaram-se as propriedades de seletividade membranar, bem como os possíveis mecanismos de ação deste novo AMP, recorrendo-se a técnicas de espectroscopia de fluorescência e de dispersão de luz. Como sistemas modelo de membranas usaram-se lipossomas (LUVs; *large unilamellar vesicles*) e, para além destes, células de *Escherichia coli*, tendo em conta que a ação deste péptido tinha sido observada para membranas aniónicas de bactérias Gram-negativas. Por um lado, a variação de intensidade de fluorescência intrínseca do péptido (possível devido à presença de um resíduo de triptofano no C-terminal) foi seguida para quantificar a inserção do péptido em membranas e testar a especificidade de ação do mesmo, tendo em conta o sistema membranar usado. A acrilamida, uma molécula capaz de extinguir a fluorescência de resíduos de triptofano, foi usada de forma a avaliar o grau de internalização deste. Sondas fluorescentes foram também testadas, quer em lipossomas, quer em células bacterianas, de forma a ser possível analisar as alterações nas diferentes propriedades membranares que o péptido provoca. Entre essas propriedades, a fluidez, o empacotamento lipídico e o potencial dipolar de membrana foram estudadas, usando para tal DPH / TMA-DPH, Laurdano e di-8-ANEPPS como sondas repórter, respetivamente. Possíveis alterações no potencial superficial membranar de vesículas e de células bacterianas foram estudadas recorrendo-se a medidas de potencial-zeta. A dispersão dinâmica de luz permitiu estudar efeitos de agregação lipídica. Em todos os estudos realizados, a constituição lipídica das vesículas foi semelhante, tendo sido escolhido com base na ação do péptido. Vesículas de POPC foram estudadas como controlo negativo da ação do péptido. De forma a mimetizar a membrana bacteriana, lipossomas de POPC:POPG (70/30), POPE:POPG:CL (63/33/4) e POPE:POPG:CL:LPS (80/16/1/3) foram testadas, com as duas últimas constituições a mimetizar as membranas externa (OML) e interna (IML) de bactérias Gram-negativas, respetivamente. Vesículas lipídicas neutras enriquecidas em colesterol, POPC:Chol (70/30), foram também testadas, mimetizando células humanas saudáveis. Comparando os resultados obtidos para todas estas vesículas, foi-nos possível elucidar a contribuição relativa que os diferentes lípidos presentes nas membranas poderão ter nas interações péptido-membrana.

Os resultados obtidos confirmaram a importância das forças eletroestáticas para a selectividade membranar do péptido *Ec*AMP1R2, que se mostrou específico para membranas aniónicas, não tendo ação em membranas neutras. Esta especificidade pode ser deduzida

directamente a partir dos resultados de partição membranar e de extinção de fluorescência, mas também observando que não promove quaisquer alterações das propriedades das membranas estudadas. Deste modo, justifica-se o facto de não ter qualquer efeito tóxico em células humanas, cujas membranas são maioritariamente neutras. Por outro lado, os resultados sugerem que a afinidade do péptido por vesículas aniónicas é maior nas que mimetizam a membrana interna e externa de bactérias. Este resultado sugere que a presença de lípidos específicos, como a cardiolipina e o LPS, poderá ser determinante para a acção do AMP. A presença de LPS surge aqui como essencial para que as interacções iniciais ocorram e promovam a interação péptido-membrana, já que é tanto nas vesículas de OML como nas células de *E. coli* que o potencial dipolar sofre mais alterações (os únicos sistemas testados na presença destas moléculas). Poder-se-á dizer que a membrana externa surge assim inicialmente como o alvo preferencial para este AMP.

Relativamente às outras propriedades membranares estudadas, a ação do *Ec*AMP1R2 não levou a nenhuma alteração de fluidez, independentemente do sistema estudado, sendo apenas possível observar uma pequena alteração do empacotamento lipídico em vesículas que mimetizam a membrana interna bacteriana (IML), sugerindo assim que este AMP é também capaz, após internalização, de atuar na membrana interna das bactérias. Curiosamente, estas vesículas foram as únicas que agregaram após um aumento crescente da concentração de péptido, embora não tenha sido seguido duma neutralização das cargas superficiais. Com base nestes dados, foi possível formular a hipótese que este AMP promove processos de fusão ou hemifusão membranar, após internalização ou destruição da membrana externa de bactérias Gram-negativas. Uma das explicações que poderá corroborar esta hipótese é o facto de lípidos com curvatura intrínseca, como é o caso da cardiolipina, favorecerem este tipo de processos.

Concluindo, os resultados obtidos ao longo deste estudo sugerem que o péptido antimicrobiano *Ec*AMP1R2 poderá ser um bom candidato para o tratamento de infeções causadas por bactérias Gram-negativas. Demonstrou-se que os modelos de membrana simples são aproximações de constituições lipídicas controláveis que permitem extrapolar, com uma boa aproximação, o modo de ação de moléculas biologicamente relevantes.

Palavras chave: Péptido antimicrobiano; *Ec*AMP1R2; interação péptido-membrana; bactérias Gram-negativas.

Abstract

Tackling antibiotic resistance is a worldwide priority. Antimicrobial peptides (AMPs) have been pointed as promising antimicrobial alternatives to conventional antibiotics. Most AMPs are cationic amphiphiles that kill bacteria by selectively attach and disrupt their negatively charged membranes. *Ec*AMP1R2 is a newly designed cationic AMP with a high antimicrobial activity against *Escherichia coli*, without being cytotoxic to mammalian cells.

Although the structure of *Ec*AMP1R2 was well characterized in preliminary work, its activity is not well understood. In this work, we tried to elucidate the membrane selectivity and membrane activity of *Ec*AMP1R2 in biomembrane models and *Escherichia coli* cells, by using optical spectroscopic techniques. Large unilamellar vesicles (LUVs) with different lipid compositions were used, including two mixtures mimicking the outer (OML) and the inner (IML) membranes of *E. coli*. Following the intrinsic fluorescence of the tryptophan residue of the peptide, it was observed that *Ec*AMP1R2 discriminates between zwitterionic (mammalian-like) and anionic (bacterial-like) membranes. The effect of *Ec*AMP1R2 on the physical properties of the membranes was monitored using diverse membrane probes. Finally, light scattering spectroscopy techniques were used to follow possible vesicle aggregation or changes in membrane surface charge due to the action of the peptide. Our results suggest that *Ec*AMP1R2 internalizes deeply inside the outer membrane of *E. coli*, causing changes in the dipole potential, but little alterations on the surface charge. Moreover, *Ec*AMP1R2 shows preferential affinity towards model membranes enriched in lipopolysaccharide, the major component of the outer membrane of Gram-negative bacteria. Additionaly, *Ec*AMP1R2 promotes the aggregation of IML vesicles, with which also demonstrates high affinity, without neutralizing the surface charge. This has led us to hypothesize that an increased selectivity of *Ec*AMP1R2 towards cardiolipin molecules of these vesicles leads to a hemi-fusion or fusion process.

Key words: antimicrobial peptides, *Ec*AMP1R2, peptide-membrane interactions, Gram-negative bacteria.

Contents

List of Figures and Tables

Symbols and Abbreviations

ACP	Anticancer peptide
AFM	Atomic force microscopy
AMP	Antimicrobial peptide
AMR	Antimicrobial resistance
ANS	8-Anilino-1-nonaphthalenesulfonic acid ammonium salt
APD	Antimicrobial peptide database
CDC	Centers for Disease Control and Prevention
ATCC	American Type Culture Collection
CL	Cardiolipin
CPP	Cell penetrating peptide
CRE	Carbapenem resistant *Enterobacteriaceae*
$\mathbf{D_H}$	Hydrodynamic diameter
di-8-ANEPPS	4-[2-[6-(Dioctylamino)-2-naphthalenyl]ethenyl]-1-(3-sulfopropyl)-pyridinium
DLS	Dynamic light scattering
DPH	1,6-Diphenyl-1,3,5-hexatriene
FP	Fusion peptide
$\boldsymbol{\gamma_L}$	Molar volume of lipids
$\boldsymbol{G_P}$	Generalized polarization
HDPs	Host defense peptides
IML	Inner membrane like vesicles
$\boldsymbol{K_d}$	Dissociation constant
$\boldsymbol{K_p}$	Partition constant
$\boldsymbol{K_{SV}}$	Stern-Volmer constant
$\boldsymbol{\lambda_{em}}$	Emission wavelength
$\boldsymbol{\lambda_{exc}}$	Excitation wavelength
LB	Luria-Bertani broth
LPS	Lipopolysaccharide
LUV	Large unilamellar vesicle
MD	Molecular dynamics simulation
MHB	Mueller Hinton broth

MIC	Minimum inhibitory concentration
OD	Optical density
OML	Outer membrane like vesicles
[*P*]	Peptide concentration
POPC	1-Palmitoyl-2-oleoyl-*sn*-glycero-3-phosphocholine
POPE	1-Palmitoyl-2-oleoyl-*sn*-glycero-3-phosphoethanolamine
POPG	1-Palmitoyl-2-oleoyl-*sn*-glycero-3-phosphoglycerol
r	Fluorescence anisotropy
SARs	Structure activity relationships
TMA-DPH	N,N,N-trimethyl-4-(6-phenyl-1,3,5-hexatrien-1-yl)phenylammonium *p*-toluenesulfonate
WHO	World Health Organization
ζ	Zeta-potential
ζ_0	Zeta-potential in the absence of peptide
ζ_X	Zeta-potential at peptide concentration X

Introduction

In the 1940s, the introduction of penicillin gave rise to the era of antibiotics, which was a breakthrough in modern medicine, allowing an effective fight against bacterial infections. However, the extensive misuse of antibiotics in livestock and in medicine has favored the emerging of antimicrobial resistance (AMR). As a result, an apocalyptic scenario in which minor infections may kill is no longer a fantasy[1]. Moreover, the thriving of antimicrobial resistant bacteria could eventually turn impossible the development of key medical procedures dependant on antibiotics (*e.g.* surgery, chemotherapy). Estimations suggest that in 2050, AMR will cause ten million deaths every year, outreaching the current mortality of cancer[1,2]. Unfortunately, the development of new antibiotic molecules is tremendously expensive and time consuming, and as a result, most of the pharmaceutical companies have left this area[3].

1. Antimicrobial peptides

Antimicrobial peptides (AMPs) represent one of the most ancient forms of defense against infection. This idea is reinforced with the fact that there have been found AMPs in all domains of life (see antimicrobial peptide database [APD][4]). In vertebrates, AMPs are included in the innate branch of the immune system. In humans, AMPs are mainly secreted by mucosal surfaces and by neutrophils[5]. In addition to their ability to kill potential pathogens, some AMPs have demonstrated immunomodulatory properties, thus being referred to as host defense peptides (HDPs)[6–8]. Likewise other components of the innate immune system, AMPs display a broad spectrum of antimicrobial activity, protecting against an extensive array of infective agents, some of them being even effective against cancer cells (anticancer peptides, ACPs)[6,9,10]. The selectivity of AMPs is dependent upon general biochemical traits that membranes of potential pathogens share. For instance, they are usually cationic, being thus prone to attach through electrostatic forces to the negatively charged membranes of bacteria. Membranes of mammalian cells, on the other hand, are neutrally charged, preventing AMPs from interacting with them through electrostatic forces.

Regarding the mode of action, it is commonly accepted that AMPs act by permeabilizing membranes, following a general pattern. Briefly, peptide molecules adsorb to the bacterial membrane through electrostatic-driven interactions. Following this, folding of the peptide

occurs facilitating the insertion of the peptide, resulting in a disturbance of the membrane[11]. The question of how the peptide causes a membrane disruption enough to kill has been studied, and some models have been proposed. The most widely accepted models are the pore formation and the detergent-like models (Figure 1). Among the most frequently identified peptide-induced pore formation mechanisms are the toroidal and the barrel-stave pore models. In the barrel-stave model, peptides insert perpendicular relative to the plane of the bilayer, forming the "staves" in a "barrel-shaped" cluster. In the toroidal model, peptides also align perpendicular to the membrane, but in this case the interaction will cause an inwards bending of the membrane, so that the bilayer also lines the pore. However, although permeabilization seems to be crucial for the peptide action, it might be insufficient to explain antimicrobial activity. Besides, the accumulation of evidences that do not fit into these models have led to the formulation of new ones, some of which will be explored later[12,13].

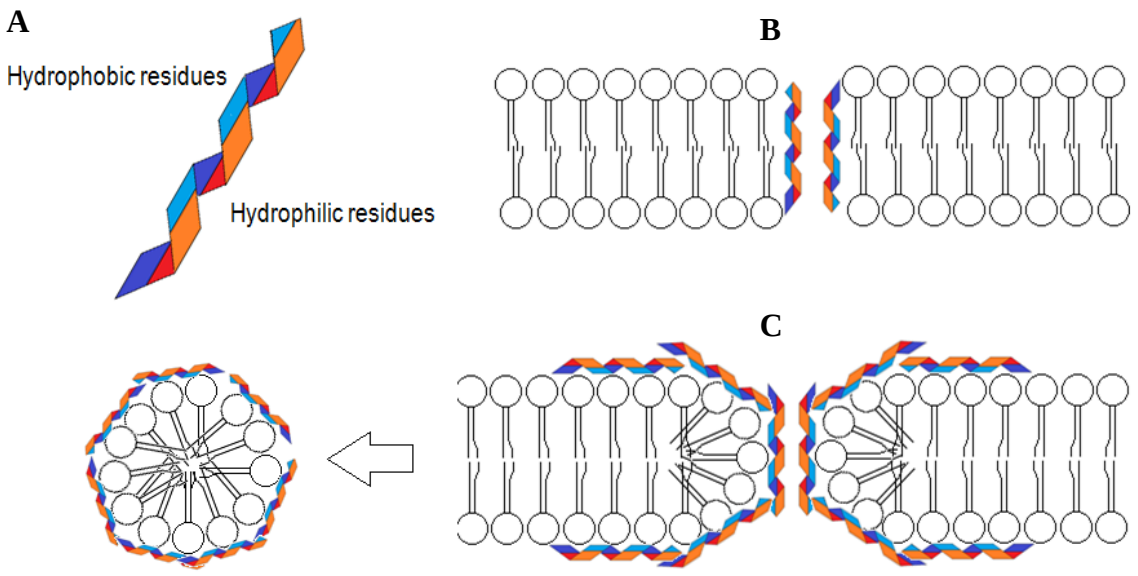

Figure 1. Mechanisms of mode of action proposed for AMP. (A) Simplified representation of an α-helical AMP. Hydrophobic residues are highlighted in blue and the cationic ones in red. (B) Pore formation: peptides insert perpendicularly in the bilayer, associate and form a pore. (C) Detergent like activity (carpet model): peptides adsorb parallel to the membrane, and after a concentration threshold is reached, they disrupt the membrane through a detergent-like mechanism, causing micellization of the membranes. (Adapted from Computational Peptidology[14])

Certain AMPs kill microbes by targeting intracellular components, namely DNA and RNA[15]. In these cases, membrane permeabilization is not necessary for the antimicrobial activity. Still, interaction with membranes is a necessary condition, because the AMP must cross the cytoplasmatic membrane in order to reach its intracellular target.

As to their clinical potential, AMPs display several desirable features. First, the already mentioned ability to kill rapidly a broad spectrum of infectious agents in the low micromolar range[16,17]. Moreover, it has been argued that bacteria will less likely develop resistance to AMPs, compared to conventional antibiotics[18]. The justification to this is that AMPs act on generalized targets such as membranes, while conventional antibiotics act upon specific targets such as bacterial enzymes. Thus, resistance to AMPs would involve such membrane rearrangements that would severely affect the bacterium fitness[18,19]. Still, as these peptides would exert selective pressures over bacteria, resistance will eventually appear, as it has been already reported[20]. However, recent studies suggest that AMPs do not elevate mutation rates as conventional antibiotics do. This confers an overwhelming advantage of AMPs over antibiotics, since mutation rate is closely related with speed of adaptation[21].

2. Molecular determinants of the membrane-AMP interaction.

AMPs are generally short peptides (10 - 50 amino acid residues) with varied amino acid composition and structure. However, most described antibacterial AMPs are random coiled when embedded in the aqueous bulk and acquire an α-helical structure upon interaction with bacterial membrane[12]. This conformational flexibility is a key property of AMPs[22]. Besides, they are generally cationic-amphipathic molecules. The positive charge of the peptide determines the selective adsorption to the anionic membranes of bacteria. Amphipathicity (*i.e.* the relative proportion and distribution of hydrophobic and polar residues within the peptide) is crucial for the mechanism of action and the secondary structure of the peptide. While cationic amino acids are responsible for the initial interaction to the membrane, hydrophobic residues are crucial for the partition of the peptide into the non-polar core of the bacterial membrane[23–25].

On the other hand, some biochemical traits of bacterial membranes are key determinants of the nature of the interaction with the peptide. Bacterial membranes have usually variable proportions of negatively charged phospholipids, such as phosphatidylglycerol or cardiolipin, being usually higher in Gram-positive bacteria[26]. In addition, some AMPs display increased affinities towards specific membrane constituents, namely the head groups of certain phospholipids[12,27,28]. Usually, the higher fluidity of bacterial membranes comparatively to the membranes of animal cells (cholesterol-enriched) makes the first more prone to disruption by the action of AMPs[29,30]. Furthermore, bacteria usually display higher transmembrane potential

(more negative in the inside), which may act as a driving force for peptide insertion and translocation. How the peptide orientates in the bacterial membrane is particularly affected by its curvature strain, which in turn depends on the shape of the lipid constituents of the bilayer[12,25,31].

Finally, the nature of the cell wall is also definitive for the bacterial susceptibility to AMPs. The Gram-positive cell wall is made up by a main thick matrix of peptidoglycan enriched in anionic molecules such as teichoic and teichuronic acids (Figure 2). AMPs take advantage of these cell wall components to reach the plasmatic membrane, although the mechanism by which they do so is not yet fully understood[12,20]. Gram-negative bacteria, conversely, have a minor peptidoglycan matrix, but possess an outer membrane, with diverse lipoproteins maintaining it anchored to the peptidoglycan layer (Figure 2). Lipid components of the outer membrane are asymmetrically distributed. The inner leaflet of the Gram-negative outer membrane has a similar lipid composition to the cytoplasmic membrane, including anionic cardiolipin and phosphatidylglycerol[32]. On the other hand, the major component of the outer leaflet is the anionic lipopolysaccharide (LPS)[33]. Many peptides have shown to self promote their uptake by displacing the native cations (Mg^{2+} and Ca^{2+}) of the LPS. Besides, being bulky, they disrupt the normal barrier of the outer membrane[34].

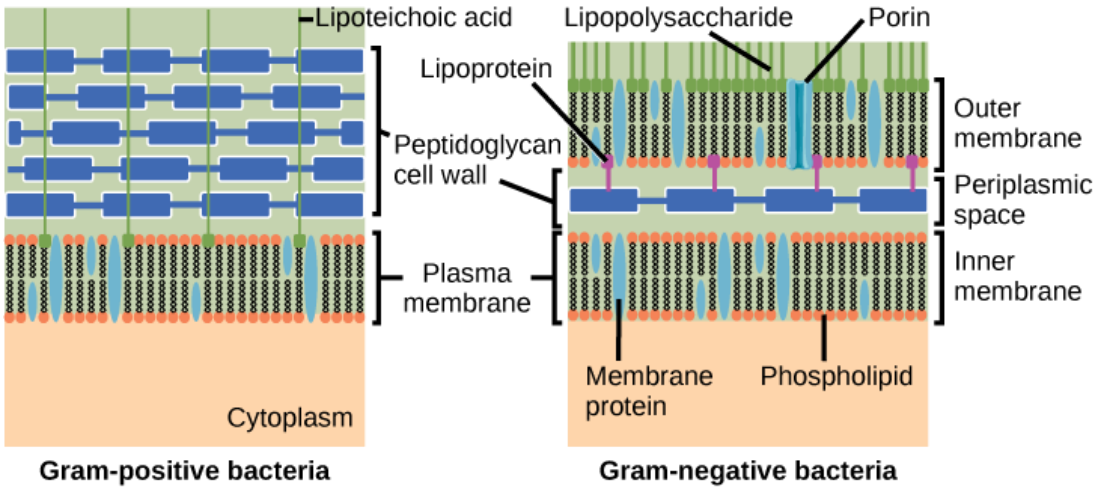

Figure 2. Scheme of the cell wall in Gram-positive and Gram-negative bacteria. The main differential components are discussed in the text (Free License)[35].

3. Design of synthetic AMPs

In spite of the initial high hopes raised by naturally occurring AMPs, they did not meet some requirements necessary to be implemented as antimicrobial agents. The main limitations of

many naturally occurring AMPs are high manufacturing costs, undesirable toxicity against host cells, poor pharmacokinetic properties and low efficiency, being some susceptible to *in vivo* proteolysis[16]. Still, AMPs have multiple attributes that makes them very convenient as potential antimicrobial drugs[36]. Being relatively small molecules, AMPs can be easily manipulated and modified. There have been extensive efforts aiming to design synthetic improved (*e.g.* shorter sequences associated to lower production costs, more potent or less cytotoxic, resistant to proteolysis) variants of AMPs[34,37]. In order to fully exploit the therapeutic potential of these molecules it is fundamental to unravel the structural determinants that govern their biological activity. Traditional approaches involved sequence modification of natural templates, and have enabled extensive progresses in the understanding of structure-activity relationships (SARs) of AMPs[38,39]. Diverse approaches have been used, based on the activity comparison between peptide variants altered in some of their properties, such as size, charge, hydrophobicity or secondary structure[12,40]. As a result, now we understand that peptide alteration in some of the biochemical properties beyond a threshold can result in drastic alterations in toxicity, stability or activity[12,19,41].

However, the operational capacity of traditional SAR-based methods is low, costly and time-consuming. In this sense, the thriving of bioinformatics has been greatly helpful. For instance, diverse AMP sequence databases have been created, such as the APD, that provide a great source of templates to work with and an *indispensable knowledge base for activity prediction models*[39]. Moreover, computational-biophysical approaches, are enhancing the predictive capacity that has allowed a radical improvement in the AMPs design[39]. Molecular modeling, for instance, is used to predict the three dimensional structure and the dynamics of a peptide[14]. Although with still some limitations, computational techniques are continually evolving, and facilitate the design procedure by allowing a sequence screening in AMP databases and the selection of a workable load of potential candidates for synthesis and experimental testing.

4. *Ec*AMP1R2: a novel synthetic cationic AMP

This work is an exploration of the biological activity of a synthetic antimicrobial peptide named *Ec*AMP1R2. This peptide was designed by the group headed by Prof. Octavio L. Franco, from Universidade Católica de Brasília and Universidade Católica Dom Bosco (Campo Grande, Brazil), with whom we have been collaborating in this project. The design of *Ec*AMP1R2 was based on a predictive bioinformatic algorithm that took into account the

properties that lead to a higher antimicrobial activity, but whose characteristics are yet unpublished. Therefore, the exact sequence of the peptide will not be detailed for the sake of respect to the intellectual property. However, some of its structural characteristics will be exposed to give a perspective as broad as possible. *Ec*AMP1R2 is an amphiphilic-cationic peptide with 19 amino acid residues and a net charge of +5. A relevant characteristic of *Ec*AMP1R2 is that it has a C-terminal tryptophan residue. Tryptophan is an intrinsically fluorescent amino acid[42], which makes it very convenient in the study of peptide-membrane interactions using fluorescence spectroscopy. Fluorescence spectroscopy techniques are among the most sensitive and suitable tools in the study of membrane active peptides[43,44]. Besides, being hydrophobic and bulky, tryptophan is also a suitable amino acid when it comes to designing antibacterial AMPs [23,45].

4.1. Preliminary results

The *in vitro* activity of *Ec*AMP1R2 was assessed, showing a relatively high antimicrobial activity against the Gram-negative bacterium *Escherichia coli* (ATCC 25922). This bacterium belongs to the family *Enterobacteriaceae*, and is a species with a large sanitary interest. Although it is a normal inhabitant of the gut, some strains contain virulence factors that makes them hazardous. Recently, carbapenem-resistant *Enterobacteriaceae* (CRE) have been included by the CDC (Centers for Disease Control and Prevention, USA) in the maximum level of concern[46,47]. Carbapenem is a last resort β-lactam antibiotic that has been used for years to treat infections of resistant *Enterobacteriaceae*, including those producing extended spectrum β-lactamases[46]. Flow cytometry studies aiming to elucidate the permeabilization ability of *Ec*AMP1R2 over time in *E. coli* (ATCC 25922) were carried out. The results showed the velocity of action of the peptide. Cytotoxicity assays for *Ec*AMP1R2 were also carried out. The results neither show hemolytic activity against human erythrocytes nor cytotoxic effects against RAW 264.7 monocyte cell line, up to the maximum concentration (200 µg/mL) used in the bioassays (unpublished data).

Using computational tools, diverse structural and functional aspects of *Ec*AMP1R2 were predicted. The adoption of a secondary structure in the presence of solvents with different polarities, predicted by molecular dynamics simulations, show a secondary structure (α-helix) loss in polar solvents, maintaining the N-terminal structured (Figure 3.A). The results of these simulations is a trajectory recording the detailed dynamics of each atom of the different molecules involved[14].

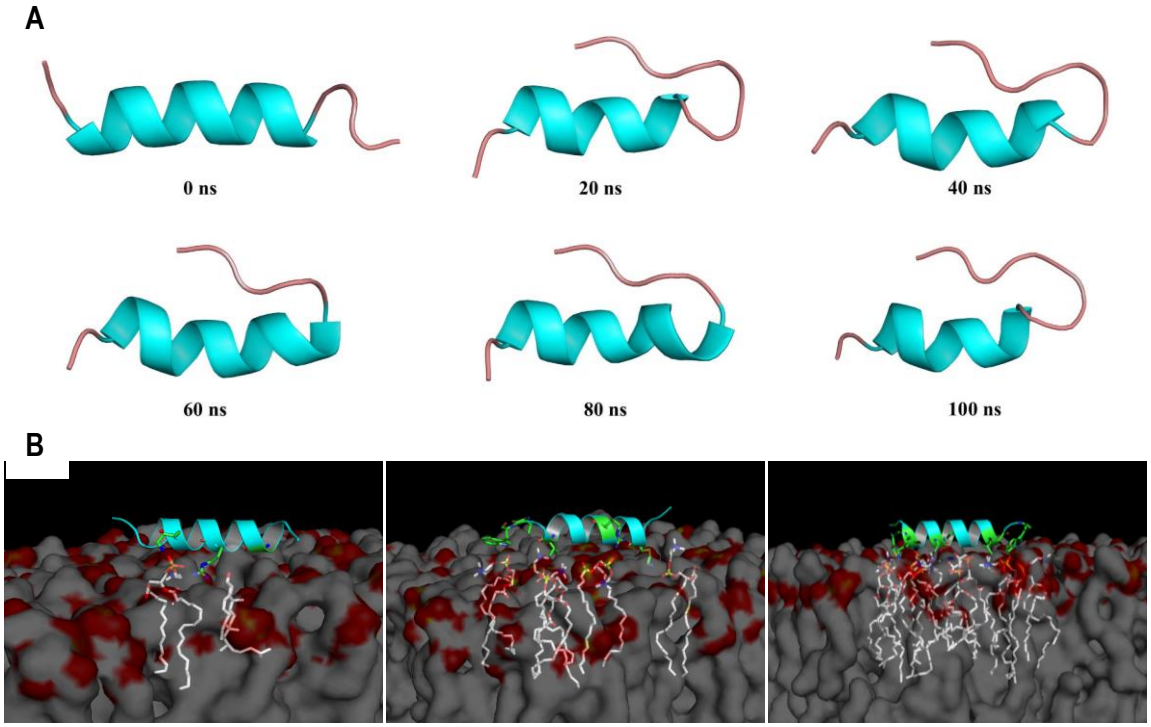

Figure 3. Snapshots obtained by molecular dynamics simulations. (A) Prediction of the secondary structure of *Ec*AMP1R2 along 100 ns, in water. (B) Prediction of the positioning (docking) of the peptide upon interaction with three membrane compositions: from left to right, POPC:cholesterol (70/30), pure POPC and POPC:POPG (70/30).

Molecular docking can predict the preferred orientation of the peptide upon interacting with membranes with diverse lipid compositions[14]. Figure 3.B represents the predicted docking of *Ec*AMP1R2 towards three membrane systems, two of them neutral (zwitterionic) and one anionic. The latter shows the higher number of atom-per-atom peptide-membrane interactions, suggesting a preference of the peptide to interact with bacterial-like models (unpublished data). Conversely, the membrane containing cholesterol (left) has the lowest score of atom-per-atom, showing that mammalian-like membranes are not the preferable target of this AMP, and suggesting a low toxicity to mammalian cells, as demonstrated in the cytotoxicity assays.

By circular dichroism, it was seen that *Ec*AMP1R2 shows an α-helical secondary structure in the presence of negatively charged lipid vesicles. The higher degree of secondary structuring was observed for vesicles of POPC:POPG (70/30), presenting a higher α-helix content, with contribution of the unstructured regions. Conversely, when the peptide is free in solution or in the presence of zwitterionic vesicles, it showed clearly a random coil behavior. These results indicate a higher affinity of *Ec*AMP1R2 towards bacterial-like membranes. Regarding the vesicles that mimic the two membranes present in Gram-

negative bacteria, the peptide adopted a β-sheet structure upon interaction with the inner-membrane like (IML) vesicles, which was not expected.

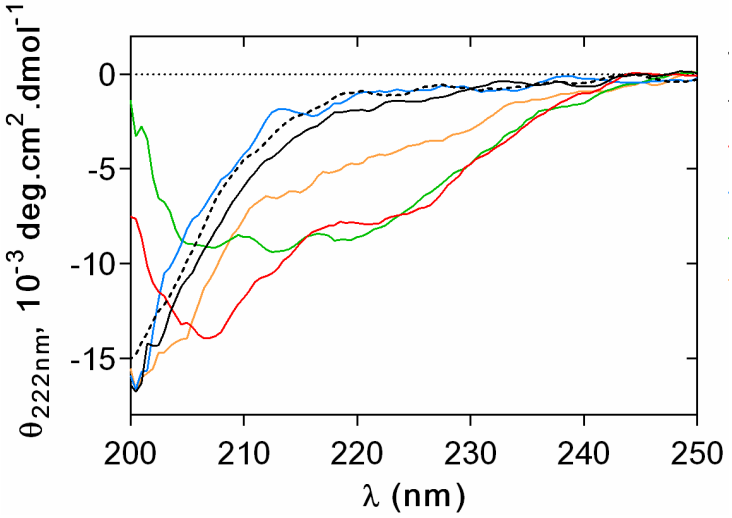

Figure 4. Conformational changes of EcAMP1R2 evaluated by Circular Dichroism in aqueous solution (---), POPC (—), POPC:POPG (70/30) (—), POPC:Chol (—), IML (—) and OML (—), with a peptide to lipid ratio of 0.002 (unpublished data).

Objectives

The main goal of the present work was to study the membrane activity and selectivity of a novel synthetic antimicrobial peptide, *Ec*AMP1R2, using biophysical approaches based on fluorescence spectroscopy and light scattering spectroscopy (DLS and Zeta-potential) techniques.

To do so, several sub-objectives were established:

1. Study the aggregation of *Ec*AMP1R2
2. Analyze the selectivity of *Ec*AMP1R2 towards bacterial-like and mammalian-like membranes, following the intrinsic fluorescence of *Ec*AMP1R2 upon interaction with large unilamellar vesicles.
3. Elucidate the alterations in membrane physical properties caused by the peptide, aiming to get insights on the mechanistic aspects of the mode of action of *Ec*AMP1R2.
4. Comparatively study the events leading to the membrane alteration in bacteria and in model system membranes.

Materials and methods

1. Materials

*Ec*AMP1R2 peptide (purity >95%) stock solutions were prepared in Milli-Q water, filtered with pore size 0.2 µm, to a final concentration of 468 µM and stored at -20 ºC. POPC (1-palmitoyl-2-oleoyl-*sn*-glycero-3-phosphocholine), POPG (1-palmitoyl-2-oleoyl-*sn*-glycero-3-phosphoglycerol) and POPE (1-palmitoyl-2-oleoyl-*sn*-glycero-3-phosphoethanolamine), were obtained from Avanti Polar Lipids (Alabaster, AL, USA). Cardiolipin sodium salt from bovine heart (CL), cholesterol (Chol), lipopolysaccharide from *Escherichia coli* O26:B26 (LPS), Luria-Bertani Agar (LB), Mueller Hinton Broth (MHB), 8-anilino-1-nonaphthalenesulfonic acid ammonium salt (ANS), Pluronic F-127, TMA-DPH (N,N,N-trimethyl-4-(6-phenyl-1,3,5-hexatrien-1-yl) phenylammonium p-toluenesulfonate) and DPH (1,6-Diphenyl-1,3,5-hexatriene) were purchased from Sigma Aldrich (St. Louis, MO, USA). The probes 2-dimethylamino-6-lauroylnaphtalene (Laurdan) and 4-[2-[6-(dioctylamino)-2-naphthalenyl]ethenyl]-1-(3-sulfopropyl)-pyridinium (di-8-ANNEPS) were obtain from Invitrogen (Carlsbad, CA, USA). Hepes 10 mM, with NaCl 150 mM, pH 7.4, was used as buffer in all experiments.

2. LUVs preparation

Large unilamelar vesicles (LUVs) were used as biomembranes model systems. In Table 1 are summarized the different vesicles used in this work, each of them mimicking diverse biological membranes.

Table 1: Lipid composition of selected model membrane systems, with their biological relevance.

Lipid composition	Biological relevance	Reference
POPC	Comparison	[27]
POPC:POPG (90/10)	Bacteria	[27]
POPC:POPG (70/30)	Bacteria	[27]
POPC:Chol (90/10)	Mammalian	[27]
POPC:Chol (70/30)	Mammalian	[27]
POPE:POPG:CL (63/33/4)	Inner membrane of *E. coli* (IM-Like)	[33]
POPE:POPG:CL:LPS (80/16/1/3)	Outer membrane of *E. coli* (OM-Like)	[33]

LUVs with approximately 100 nm of diameter were prepared by extrusion[48]. Initially, lipids were dissolved in Choloroform in a round-bottomed flask. For LPS lipid film formation, LPS was dissolved in a mixture Choloroform/methanol 2:1 and the solution was extensively vortexed and bath sonicated, at 40 ºC, during 15 min. After mixing, lipids were dried under a stream of nitrogen, forming a thin lipid film in the flaks wall, and left overnight under vacuum. The dried lipid mixtures were then re-hydrated in buffer. The resulting solution was frozen and thawed eight times, resulting in the formation of multilamellar vesicles (MLV). Finally, LUVs of approximately 100 nm were obtained by extrusion, using a LiposoFast-Basic (Avestin Europe, Mannheim, Germany). For most of the different lipids or lipid mixtures, extrusions were done 21 times, through a polycarbonate membrane with a pore size of 100 nm (Whatman, Florham Park, NJ, USA). For OML and IML vesicles, extrusion was done 41 times, since control size determinations by dynamic light scattering spectroscopy showed that a higher number of extrusion cycles was necessary to achieve the size distribution characteristic of LUV[48].

3. Bacterial culture

An aliquot of 10 µL of *Escherichia coli* ATCC® 25922™, obtained from American Type Culture Collection (ATTC, Manassas, VA, USA), was plated on LB agar, and incubated overnight, at 37 ºC. An isolated colony was re-suspended into 5 mL of MHB and grown overnight at 37 ºC, until the log-phase state is reached. A 100 µL inoculate was transferred into 5 mL of fresh medium and grown 3 h, then centrifuged 4000 g, for 25 min, at 10 ºC, and washed three times with MHB medium. The optical density at 600 nm ($O.D._{600nm}$) of bacteria was adjusted in order to obtain a cell density of approximately 1×10^6 cells/mL[49].

4. Fluorescence spectroscopy measurements

Fluorescence measurements were carried out in a Varian Carry Eclipse fluorescence spectrophotometer (Mulgrave, Victoria, Australia) equipped with a Xenon pulsed lamp. The spectral bandwidths of excitation and emission were of 5 nm and 10 nm, respectively. These bandwidths were used in all fluorescence spectroscopy studies. Fluorescence spectra were recorded with 0.5 cm path length quartz cells. All measurements were performed at least three times with independent measurements, at 25 ºC. All fluorescence spectra were corrected for lipid scattering and dilution effects.

4.1. Peptide aggregation assay by ANS

Anilinonaphthalenesulphonates are non-fluorescent in polar environments, and become fluorescent when embedded in the hydrophobic core of proteins. This property makes them sensitive indicators of processes that modify the exposure of the probe to water, such as protein aggregation[50]. The aggregation of *Ec*AMP1R2 was followed by measuring ANS fluorescence intensity, with an excitation wavelength (λ_{exc}) of 380 nm and emission wavelengths (λ_{em}) between 400 and 650 nm. ANS (25 µM) in buffer was titrated with a range of *Ec*AMP1R2 concentrations from 0 to 30 µM. The behavior of the fluorescence intensity (with λ_{em} at 480 nm) against peptide concentration was analyzed, as well as possible displacements in the ANS emission spectrum towards lower wavelengths[51].

4.2. Partition coefficient determination

Fluorescence techniques are among the most sensitive and very suitable when quantifying the partitioning of a peptide into membranes. The insertion of a fluorescent residue of a peptide in a lipid membrane leads to a change of its quantum yield (usually increasing)[42,44,52]. This property can be used to determine the partition constant or partition coefficient (K_p) of the peptide between the aqueous and the lipid phases. To study the partition of the peptide between the lipid and the aqueous phase, lipid mixtures of different compositions were used. Peptide partitioning into lipid bilayers was monitored by registering changes in the peptide intrinsic tryptophan fluorescence upon addition of lipid vesicles. Successive aliquots of LUVs were added to a peptide solution (6 µM). After each addition of small quantities of lipid (20 mM stock solutions), the sample was incubated for 5 min before recording the emission spectrum. Fluorescence emission spectra between 300 and 500 nm were recorded with excitation at 280 nm, before and after each addition of lipid. Besides, non-partitioning free tryptophan was titrated under the same experimental conditions[53]. To quantify the extent of the membrane incorporation, the partition coefficient, K_p, was calculated from the fit of experimental data using equation 4.1

$$\frac{I}{I_W} = \frac{1+K_p\,\gamma_L \frac{I_L}{I_W}[L]}{1+K_p\gamma_L[L]} \qquad 4.1$$

where I_W and I_L are the fluorescence intensities in the water and in the lipid phase, respectively, γ_L is the lipid molar volume and [L] is the lipid concentration[43].

Exceptions to the general rule of hyperbolic variation of the fluorescence intensity of a fluorophore as a function of lipid concentration can occur, mainly due to processes of self-quenching upon insertion in the membrane. When such behaviors were observed, the partition constant was calculated using equation 4.2:

$$\frac{I}{I_W} = \frac{K_p \gamma_L [L] I_L}{1 + K_p \gamma_L [L] + k_2 K_p I_L} + \frac{I_w}{1 + K_p \gamma_L [L]} \qquad 4.2$$

where k_2 is proportional to the ratio between the bimolecular self-quenching rate and the radiative decay rate[54].

5. Fluorescence quenching assays

The exposure of the Trp residue to the aqueous environment was evaluated by fluorescence quenching with acrylamide. Acrylamide is a small polar molecule commonly used as a tryptophan quencher[42]. Lipid bilayers are impermeable to acrylamide molecules because of its polarity. Hence, the fluorescence of a Trp residue inserted in a membrane system is not susceptible of being quenched by acrylamide molecules. Conversely, if quenching occurs, one can infer that the Trp residue was not inserted into the hydrophobic core of the lipid bilayer[42].

Successive aliquots of acrylamide (1 M) were added to a peptide solution in the absence and presence of vesicles ([L] = 3 mM). Emission of tryptophan was monitored between 305 and 500 nm after excitation at 290 nm, in order to minimize the quencher/fluorophore light absorption ratios. The extension of linear quenching of the tryptophan residue was quantified using the Stern-Volmer equation (5.3):

$$\frac{I_0}{I} = 1 + K_{SV}[Q] \qquad 5.3$$

where I_0 is the fluorescence intensity of the peptide measured in the absence of the quencher, I is the fluorescence intensity at a given quencher concentration, Q is the concentration of quencher (acrylamide), and K_{SV} the Stern-Volmer constant.

When a negative deviation to linear behavior is observed, experimental data were fitted using equation 5.4:

$$\frac{I_0}{I} = \frac{1 + K_{SV}[Q]}{(1 + K_{SV}[Q])(1 - f_B) + f_B} \qquad 5.4$$

where f_B is the fraction of light arising from the fluorophores accessible to the quencher[55].

6. Membrane probes

The use of fluorescence spectroscopy in the study of peptide-membrane interactions may follow two approaches. When the peptide has at least one tryptophan residue, it is possible to follow its intrinsic fluorescence, which is very informative since it is highly dependent on variations in its surrounding microenvironment[42]. Nonetheless, this approach cannot be used when the aim is to characterize the interactions of peptides with cell membranes. Cells are rich in proteins, most of them containing tryptophan residues, thus, unabling a proper following of the intrinsic fluorescence of the peptide. In the present study, sensitive probes were used as reporters of variations in membrane properties. These probes undergo some physical changes that are measurable by monitoring their spectral characteristics. In this study, four fluorescent probes (see below) were assessed to monitor the effect of *Ec*AMP1R2 on several physical-chemical properties of the membranes, both in model membranes and in *E. coli* cells.

LUVs assays with the fluorescent probes were carried out following this general scheme, with some variations in the case of the probe di-8-ANEPPS. Vesicles obtained by extrusion were labeled with the desired probes, with a probe to vesicle ratio of 1:300, and with a final concentration of lipid of 3 mM, unless otherwise indicated. The labeling process was performed with constant agitation for 30 min (60 min for di-8-ANEPPS). After labeling, aliquots of peptide were added to the mixture and incubated for 1 h.

Bacteria studies with fluorescent probes followed a similar general scheme. A suspension of *E. coli* washed three times with MHB medium and a cell density adjusted to 1×10^4 cells/mL. Then, cells were labeled with the probe to a final dye concentration of 10 µM (100 µM for di-8-ANEPPS in bacteria), during 30 min in the dark (60 min for di-8-ANEPPS). After labeling, successive aliquots of increasing concentrations of peptide were added, in a range of 0 to 20 µM and incubated for 1 h.

6.1 Laurdan assay

Laurdan is a solvatochromic fluorescent dye, whose emission spectrum is highly sensitive to the level of water penetration into the lipid bilayer. This makes Laurdan very suitable in the evaluation of changes in the lipid order (or packing) of membranes. Hence, possible changes

in the packing of lipids in bacterial cell membranes and in model membranes upon addition of peptide were monitored using Laurdan. Labeled samples were excited at 350 nm, and the emission spectrum between 400 and 600 nm was recorded. To quantify the spectral changes, the Laurdan generalized polarization (G_P) was calculated as follows:

$$G_P = \frac{I_{440} - I_{490}}{I_{440} + I_{490}} \qquad 6.5$$

where I_{440} and I_{490} are the intensities at λ_{em} 440 and 490 nm, respectively[56].

6.2 DPH and TMA-DPH assays

Changes in the fluidity of the used model membranes and bacteria cells, due to the action of the peptide were followed monitoring the anisotropy of the fluorescent probes DPH and TMA-DPH, at 25 ºC.

Polarization measurements are based in the principle of photo-selective excitation of fluorophores by polarized light (*i.e.* fluorophores preferentially absorb photons whose electric vectors are aligned parallel to their transition moment). Polarization measurements reveal the average angular displacement (rotational rate) of the fluorophore that occurs between absorption and subsequent emission of a photon. In the context of membranes, the rotational rate of a fluorophore is dependent on the fluidity of the bilayer, thus, a change in the fluidity of membranes will result in alterations in fluorescence anisotropy, being higher in bilayers in the gel phase and lower in liquid-crystal state membranes (less and more fluid membranes, respectively)[42]. Due to their location in the membrane, DPH assesses the fluidity at the hydrophobic core of the lipid bilayer, namely at the level of the fatty acid chains of the phospholipids, while its cationic derivative TMA-DPH anchors to the water/lipid interface, reporting the fluidity closer to the membrane surface[57].

Fluorescence anisotropy measurements of the samples were conducted as a function of the concentration of peptide, using a λ_{exc} of 350 nm and a λ_{em} of 432 nm in the case of DPH and a λ_{exc} 355 nm and a λ_{em} of 432 nm for TMA-DPH. Anisotropy (r) values were calculated using equation 6.6:

$$r = \frac{I_{VV} - G\, I_{VH}}{I_{VV} + 2\, G\, I_{VH}} \qquad 6.6$$

where I_{VV} and I_{VH} are the fluorescence intensities when the angle between excitation and emission polarizers are 0º (vertical) and 90º (horizontal), respectively, and *G* is the ratio of the sensitivities of the detection system for vertically and horizontally polarized light [42], being determined by

$$G = \frac{I_{HV}}{I_{HH}} \qquad 6.7$$

where I_{HV} is the fluorescence intensity with horizontally polarized excitation and vertically polarized emission, while I_{HH} is the fluorescence intensity with horizontally polarized excitation and emission.

6.3 Di-8-ANEPPS assay

Dipolar potential of membranes originates from the alignment of the polar heads and glycerol-ester regions of lipids and oriented water molecules hydrating the outer surface of the membrane[58]. Peptide insertion and electrostatic interaction will perturb the membrane dipolar potential, which can be monitored by means of a spectral shift in the excitation spectra of the probe di-8-ANEPPS. This dye incorporates in the outer leaflet of the membranes, and is sensitive to the local dipole potential by shifting its excitation spectrum[59,60]. Thus, changes in the dipole potential due to the interaction of *Ec*AMP1R2 with model membranes (bacteria and LUVs) were assessed using the dye di-8-ANEPPS.

In the case of *E. coli*, the cell suspension was prepared in buffer supplemented with 0.05 % Pluronic F-127 yielding a final cell density of 10^5 cells/mL. Then, this suspension was labeled with the dye (final concentration of 100 μM). Labeled cells were incubated for 1 h, after which aliquots of peptide were added and the excitation spectra measured with a λ_{em} of 670 nm. The effect of the peptide over the dipole potential was quantified using the ratio of fluorescence intensities at 455 nm and 525 nm (R)[60]. The ratio R allows a quantitative analysis of the variation of the dipole potential, by quantifying the shift in the excitation spectrum. The experimental results from the measurements as a function of *Ec*AMP1R2 concentration were fitted to equation 6.8:

$$\frac{R}{R_0} = \frac{\frac{R_{min}}{R_0}[\mathrm{P}]}{K_d + [\mathrm{P}]} \qquad 6.8$$

with R values normalized for R_0, the value without addition of peptide, and being R_{min} the minimum asymptotic value for R and K_d the apparent dissociation constant[58].

7. Light scattering spectroscopy

Light scattering measurements were carried out in a Malvern Zetasizer Nano ZS (Malvern, UK) with a backscattering detection at a constant scattering angle of 173º, equipped with He-Ne laser (λ = 632.8 nm). The samples were left equilibrating for 15 min at 25 ºC. Measurements were performed three times except for IML and OML LUVs, which were assessed twice.

7.1 Dynamic light scattering measurements

AMPs can induce membrane aggregation and even membrane fusion[61]. Vesicle aggregation is driven by electrostatic forces exerted by oppositely charged peptides, and has been profusely studied due to its theoretical, biological and biotechnological interest[61]. Thus, changes in the size distribution of LUVs due to the addition of the peptide *Ec*AMP1R2 were determined by Dynamic Light Scattering (DLS).

The measured diffusion coefficient (D) values were used for the calculation of the hydrodynamic diameter (D_H), through the Stokes-Einstein relationship:

$$D = \frac{\kappa T}{3\pi\eta \mathrm{D_H}} \qquad 7.9$$

where η is the dispersant viscosity, κ the Boltzmann constant and T the absolute temperature. The hydrodynamic diameter was obtained from an average taken from 15 measurements with 10 runs each[62].

For the measurements, 1 h before, aliquots of *Ec*AMP1R2 were added to a suspension of vesicles with a concentration of 200 µM diluted in HEPES buffer (pH 7.4). Buffer was previously filtered with nylon filters with a pore diameter of 100 nm, in order to reduce the amount of particles that could contribute for the scattering of the sample.

7.2 Zeta-potential measurements

Charged particles in a suspension (*e.g.* vesicles, cells or nanoparticles) attract ions to their surface, forming a layer denominated the Stern layer. Outside the Stern layer, there is another

layer where ions diffuse more freely. Within this diffuse layer there is a notional boundary inside which the particle forms a stable entity. In the presence of an electric field, the particle moves and the ions within this boundary move along with it. Conversely, ions beyond do not move concomitantly. The electric potential that exists at this boundary is called the zeta potential (ζ). This potential can be determined by measuring the electrophoretic mobility of the particles in solution towards the electrode of opposite charge in the presence of an electric field[62].

In order to evaluate the changes in the surface charge, ζ measurements were performed in *E. coli* cells and LUVs using disposable folded capillary cells with golden electrodes (Malvern, UK). Successive aliquots of peptide were added into solutions containing either bacteria (1 x 10^6 cells/mL) or LUVs (200 μM) diluted in filtered HEPES buffer. These suspensions were incubated during 1 h before the measurements. The viscosity and refractive index values were set to 0.8872 cP and 1330, respectively, and the electric field was 40 V. The electrophoretic mobility values allowed us to calculate the zeta-potential (ζ) using the Smoluchowski equation:

$$\zeta = \frac{4\pi\nu u}{\varepsilon} \qquad 7.10$$

where u is the electrophoretic mobility, ε is the dielectric constant and ν is the molar volume[62]. Each zeta-potential value was obtained from an average of 15 measurements with 100 runs each.

Results and discussion

1. Peptide aggregation studies

Because *Ec*AMP1R2 is a synthetic rationally-designed peptide, its tendency to form aggregates ought to be assessed, since ignored peptide aggregation would lead to misinterpretation of further results. Hydrophobic interactions have a great contribution in the early stage of protein aggregation[63]. We took advantage of this feature using ANS, a fluorescent dye that binds to the hydrophobic pockets in protein aggregates. When ANS is buried in an hydrophobic environment, its quantum yield (assessed through fluorescence intensity measurements) increases, and its emission spectrum undergoes a blue shift[51]. Figure 5A shows the normalized fluorescence spectra of ANS at three different peptide concentrations. Neither blue shift was observed, nor the titration of *Ec*AMP1R2 with ANS caused an increase on the fluorescence intensity (Figure 5B), suggesting that aggregation of *Ec*AMP1R2 does not occur in the experimental conditions used.

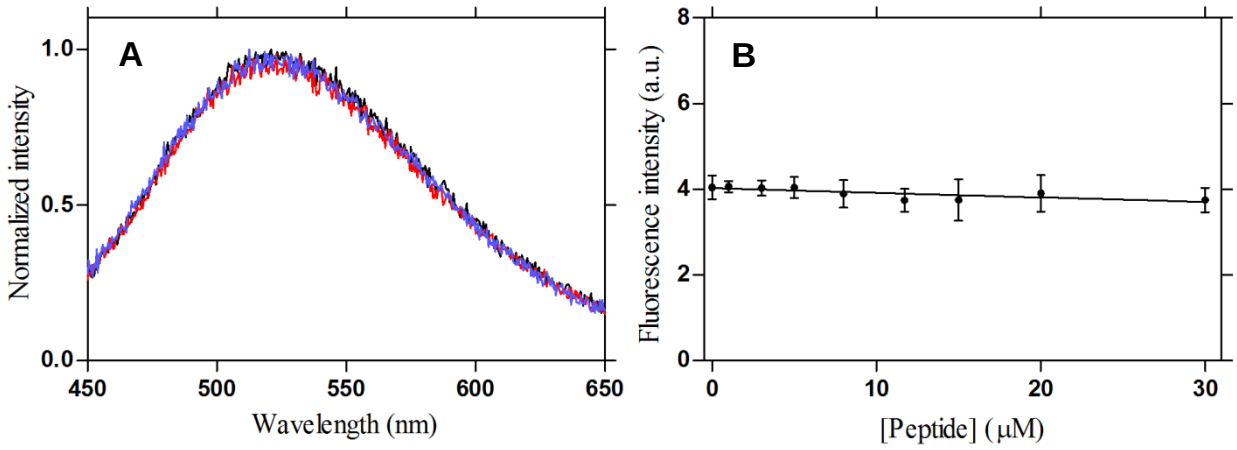

Figure 5. Aggregation studies of *Ec*AMP1R2 by ANS fluorescence (A) Fluorescence intensity of ANS (λ_{exc} = 380 nm, λ_{em} = 480 nm) spectra at three different *Ec*AMP1R2 concentrations: — 0 μM; — 11.7 μM; — 30 μM. (B) Normalized fluorescence intensity at different peptide concentrations.

2. Membrane incorporation studies with LUVs: characterization of the selectivity of *Ec*AMP1R2

AMPs are known for usually having membranes as their primary cellular target[34]. Their selectivity against bacterial membranes is generally determined by electrostatic-driven

interactions between the negatively charged polar heads of the phospholipids and the cationic residues of the peptide. These electrostatic interactions are generally weaker with mammalian cell membranes, given the zwitterionic nature of the lipids that make up the outer leaflet of these membranes[12].

The determination of the partition coefficient is a starting point in the characterization of interactions between AMPs and model membrane systems[43]. By doing this, it is possible to address the selectivity of the peptide towards bacterial-like membranes, and the extent to which the electrostatic interactions are important for the internalization of the peptide. Being both sensitive and noninvasive, fluorescence spectroscopy-based techniques are convenient to measure the partitioning of peptides that bear an intrinsic fluorescent residue. In general, the quantum yield of a tryptophan residue increases when it incorporates into a hydrophobic environment (*e.g.* when it incorporates into the non-polar core of a lipid bilayer)[42]. This feature allows the determination of the partition coefficient, K_p, using equation 4.1 for the fitting to the experimental data[43,44]. Thus, we can quantitatively evaluate the membrane selectivity of *Ec*AMP1R2, by determining its partition to vesicles with diverse lipid compositions. The LUVs tested intended to mimic the membranes of mammalian cells, a general model for bacterial cells, and the outer and inner membranes of *Escherichia coli* (here abbreviated as OML and IML, respectively). Mammalian cell membranes are rich in neutral phospholipids (such as POPC) and have cholesterol as a distinctive sterol[29]. On the other hand, bacterial cells in general are negatively charged, with variable concentrations of anionic lipids such as POPG or cardiolipin[64].

Figure 6 shows the partition curves obtained by following the intrinsic fluorescence of *Ec*AMP1R2 upon addition of successive aliquots of LUVs of pure POPC, POPC:POPG (90/10 and 70/30), POPC:Chol (90/10 and 70/30), IML and OML (see Table 2). Moreover, Table 2 shows the partition parameters obtained, K_p and I_L/I_W, for *Ec*AMP1R2, as well as the values of blue shift. Here, the blue shift of the emission spectrum towards lower wavelengths occurred when tryptophan incorporates into less polar environments[42]. The parameter I_L/I_W is the ratio between the intensity of the peptide in the lipid and in the water phase. It reflects the change of the fluorescence quantum yield of the tryptophan upon membrane insertion, providing thus valuable information[54].

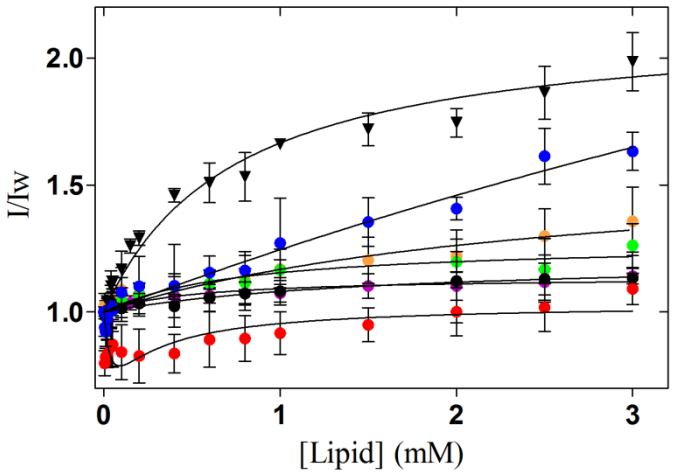

Figure 6. Partition curves of *Ec*AMP1R2 (6 µM) in five different membrane model systems: ● POPC; ● POPC:POPG (90/10); ▼ POPC:POPG (70/30); ● POPC:Chol (90/10); ● POPC:Chol (70/30); ● IML; ● OML. Lines depicted represent the adjustment of the experimental data to Equation 4.1, in the case of POPC, POPC:POPG (90/10 and 70/30), POPC:Chol (90/10 and 70/30) and OML vesicles. Non-hyperbolic behaviors (due to self-quenching processes) were adjusted to the Equation 4.2, only for IML vesicles. Fitted parameters are summarized in Table 2.

Table 2. Partition parameters and blue shift values of the peptide for each membrane model system. Values are presented as mean ± standard error (SE)

Lipid composition	K_p	I_L/I_W	Blue shift (nm)
POPC	2617 ± 741	1.14 ± 0.01	0
POPC:POPG (90/10)	508 ± 222	1.60 ± 0.15	1
POPC:POPG (70/30)	1801 ± 284	2.15 ± 0.06	11
POPC:Chol (90/10)	1794 ± 573	1.27± 0.03	0
POPC:Chol (70/30)	948 ± 345	1.21 ± 0.04	0
Inner-like	21798 ± 8485	-	5
Outer-like	101 ± 95.92	4.63 ± 2.969	8.5

The quantum yield of the tryptophan increased upon titration with most lipid compositions. An exception to this is observed for the vesicles mimicking the inner membrane of *E. coli* (IML). A plausible explanation for this is that, after interaction with membranes, the Trp residue could suffer self-quenching (due to the low lipid concentration) or quenching induced by the microenvironment where it is inserted. Considering that all systems tend to reach an equilibrium, initially, the amount of tryptophan available for interaction can be higher than usual, leading to a two-phase behavior. Also, the fact that the neighboring amino acids are

mostly lysine residues, whose side chains are natural quenchers for Trp, can be an additional cause for this exception[42]. In this case, the partition constant was determined using equation 4.2, obtaining the highest K_p compared to the other lipid compositions (see Table 2). Unexpectedly, we obtained a high K_p in pure POPC vesicles. However, some facts question the validity this value. First, regarding I_L/I_W, the low value of this parameter indicates that most peptide remains in the water phase. As a result, an accurate fitting becomes hard to accomplish, yielding elevated errors. As a matter of fact, standard error represents 28 % of the K_p value calculated. Besides this, no blue shift was observed. This explanation also applies to the similar situation that we see in the case of POPC:Chol (90/10) vesicles, in which high K_p is associated to an error of 32 %. The K_p obtained for *Ec*AMP1R2 in POPC:POPG (70/30) vesicles is among the highest values and a significant blue shift was observed. However, the K_p of the POPC:POPG (70/30) vesicles was lower than for IML. This might be caused by differences in composition, since specific membrane constituents might alter the affinity of the AMP (See Introduction Section 2). In this case, both POPE and CL (zwitterionic and anionic, respectively) might be playing an important role in such improvement in the affinity of *Ec*AMP1R2. In contrast, POPC:POPG (90/10) mixtures (slightly anionic) displayed a low K_p and a low displacement of the emission spectrum. Finally, we obtained a very low K_p when studying the interaction of the peptide with OML, with a significant error associated. The reason to this is that the equation could hardly fit the experimental results, which followed a close-to-linear behavior. In spite of this, blue shift was observed, implying that interaction actually occurred. Moreover, supporting this idea is the fact that this mixture displayed the highest I_L/I_W value.

All in all, the results aim to a low interaction of *Ec*AMP1R2 with zwitterionic (neutral) lipids, but further tests were needed to elucidate this question. On the other hand, partition studies with *Ec*AMP1R2 aim to a higher affinity towards the composition containing POPE and CL (*i.e.* those that mimic the inner membrane of *E. coli*), highlighting the importance of the use of realistic membrane model systems.

3. Exposure of the tryptophan residue to the aqueous environment

Fluorescence events are very informative about the microenvironment of a given fluorophore. Complementary to the membrane incorporation studies, quenching assays were performed. Because membranes are impermeable to acrylamide, the fluorescence of a tryptophan residue

fully inserted in a membrane is not susceptible of being quenched by acrylamide. Conversely, when an acrylamide molecule encounters with Trp, collisional (or dynamic) quenching occurs, hindering the fluorescence emission[42]. Figure 7 shows the Stern-Volmer plots obtained for *Ec*AMP1R2 in the absence and presence of vesicles. Stern-Volmer constants (K_{SV}) were calculated fitting the linear plots using equation 5.3, or using equation 5.4 when a nonlinear behavior was observed. K_{SV} values are presented in Table 3.

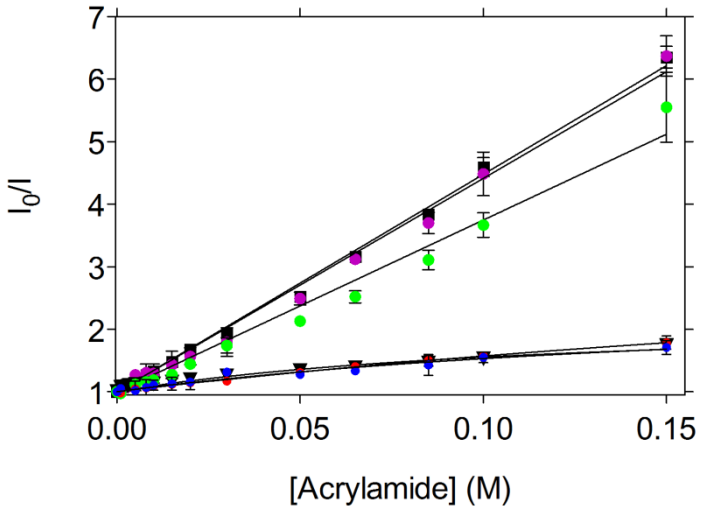

Figure 7. Stern-Volmer plots for EcAMP1R2 (6 µM) in aqueous solution (●), pure POPC (●), POPC:POPG (70/30) (▼), POPC:Chol (●), IML (●) and OML (■), at constant lipid concentration (3 mM). Solid lines represent the fitting of the data to Equation 5.3 in case of the aqueous solution, pure POPC and POPC:Chol (70/30), or Equation 5.4 in the case of POPC:POPG (70/30), IML and OML vesicles. Fitted parameters are summarized in Table 3.

Table 3: Parameters obtained for the quenching of *Ec*AMP1R2 by acrylamide in aqueous solution (free) and in the presence of lipid vesicles.

Lipid composition	K_{SV} (M^{-1}) ± S.E.	f_B
Aqueous solution	34.8 ± 1.7	-
POPC	34.1 ± 2.5	-
POPC:POPG (70/30)	18.6 ± 4.2	0.047
POPC:Chol (70/30)	27.5 ± 3.6	-
IML	9.4 ± 0.7	0.028
OML	13.1 ± 3.2	0.066

High values of K_{SV} are indicative of an efficient quenching of tryptophan fluorescence by acrylamide (a collisional quencher). As expected, the highest value of K_{SV} was obtained for the free peptide. An almost equal value was observed in pure POPC vesicles, followed by POPC:Chol (70/30). These results indicate that a low internalization of the tryptophan residue occurs in the presence of zwitterionic vesicles, and hence, can be used as a counterbalance of the partition results. The lowest K_{SV} was obtained for IML vesicles, in good agreement with what was found in the partition experiences. Low K_{SV} values were also obtained for OML vesicles, indicating that *Ec*AMP1R2 hides strongly from the quencher molecule. Also, a foreseeable low K_{SV} was observed for POPC:POPG (70/30) vesicles, corroborating a strong peptide-membrane interaction. Interestingly, we found non-linear behaviors in the three anionic model membrane systems analyzed. Nonlinear Stern-Volmer plots are indicative that two sub populations are present, each of them with different accessibility to the quencher. This means that the peptide reached a stagnation in the incorporation in the membrane, being one population protected and the other staying accessible to the collisional quencher. All results together show that *Ec*AMP1R2 has a high affinity only towards anionic membranes.

4. Changes in membrane properties: lipid fluidity, lipid packing and dipole potential.

We assessed four fluorescent membrane probes that provide information about three major properties of membranes: lipid order or packing, microviscosity or fluidity, and the dipole potential. The aim of this is to infer some functional information about *Ec*AMP1R2 action. Besides, membrane probes are not cytotoxic allowing us to analyze the properties of membranes in biological samples. Therefore, in addition to the vesicles with various compositions (pure POPC, POPC:POPG (70/30), POPC:Chol (70/30), IML and OML), we also analyzed the disturbance caused by *Ec*AMP1R2 in membranes of *E. coli* cells. This enables the comparison of the results obtained with model membrane systems, with those obtained for living cells. However, cell membranes are dynamic and heterogeneous systems, sometimes hindering the reproducibility of the experiences. Moreover, the two membranes of *E. coli* cells add more difficulties to the correct interpretation of the results. That is why, in spite of their simplicity, model membranes systems such as LUVs are convenient for these studies, in addition to the possibility of testing with them biomembrane models with different lipid compositions.

4.1 Changes in membrane packing assessed by generalized polarization

Being sensitive to the hydration level of lipid bilayers, Laurdan is useful when it comes to measure the lipid packing of membranes, allowing us to observe changes that occur in terms of lipid rearrangement. The emission maximum of Laurdan is near 440 nm in gel-phase membranes (more packed) and near 490 nm in liquid phase membranes (less packed)[65]. Generalized polarization (G_P, see equation 6.5) relates quantitatively these spectral changes. Membranes with less packed lipids will have a G_P value closer to -1, while those with G_P values closer to +1 will have more tightly packed lipids. Figure 8 shows G_P values upon increasing concentrations of *Ec*AMP1R2, for different lipid compositions.

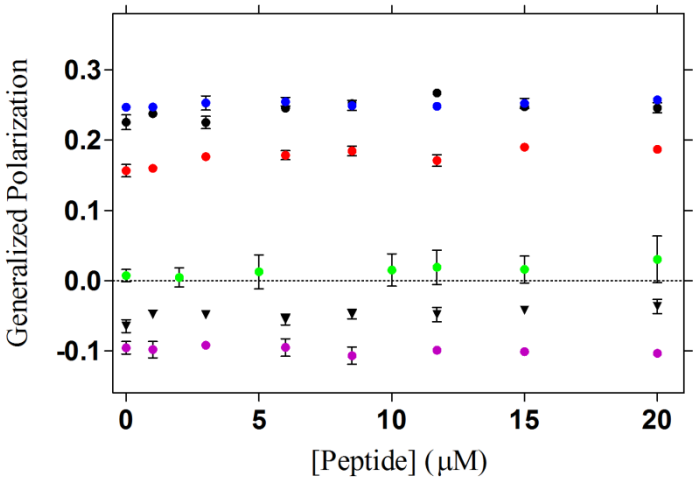

Figure 8. Generalized polarization of Laurdan (9.9 μM) as a function of *Ec*AMP1R2 concentration for POPC (●), POPC:POPG (70/30) (▼), POPC:Chol (70/30) (●), IML (●), OML (●), and *E. coli* cells (●). Lipid concentration was kept constant at 3 mM, and cell density was 1×10^5 cells/mL.

Initially, considering the G_P value for the different membranes tested without the presence of peptide, pure POPC, POPC:POPG (70/30) and *E. coli* were the samples with less packed membranes, while POPC:Chol, OML were the more tightly packed membranes, with the IML membrane showing an intermediate value, among the systems tested. Cholesterol acts as a fluidity and packing buffer[66,67]. Hence, we interpret that the loosely packed LUVs of pure POPC have been condensed by the presence of cholesterol. The high packing showed by OML vesicles might be due to the presence of LPS, which forms highly packed domains[68]. Besides, the anionic phospholipid POPG has a vesicle-condensing ability, as it can be deduced by the differences found in G_P between pure POPC vesicles and POPC:POPG mixtures, being the latest one more packed. POPG is also a major component of IML (33 %), explaining the high values of G_P. Moreover, POPE:POPG mixtures have been reported to

increase membrane packing due to the POPG umbrella effect that promote the small ethanolamine of POPE to slip underneath the large glycerol head group[69]. The difference of lipid order observed between IML and OML vesicles, besides the LPS presence in the latter, might be due to the higher concentration of CL in IML vesicles. High concentrations of CL are known to increase membrane fluidity and decrease lipid packing [70].

Apparently, the interaction of *Ec*AMP1R2 caused little or no changes in the lipid packing of the vesicles, as shown in Figure 7. Although there is an apparent increase in the lipid order of *E. coli* membranes as the peptide concentration increases, statistical analysis showed no significant differences between the initial and last concentration tested. The increased complexity of biological samples, structural changes, physiological variations, and acclimatization processes can cause higher deviations than studies with membranes systems. *Ec*AMP1R2 caused a slight increase in the G_P of IML vesicles, reporting an increase in its lipid packing, whereas no effect was observable in OML. The insertion of *Ec*AMP1R2 also causes a thickening in POPC:POPG (70/30) LUVs. A plausible explanation to this could be that the partition of the peptide into the core of the membrane could cause the exclusion of some water molecules in this area. However, this question will be further addressed, taking into account the overall changes caused by *Ec*AMP1R2.

4.2 Changes in membrane fluidity assessed fluorescence anisotropy

Anisotropy measurements provide information about the rotational diffusion of the fluorophore. The rotational rate of fluorophores in membranes depend on membrane fluidity. Thus, the effect in membrane fluidity of vesicles and *E. coli* cells upon successive additions of *Ec*AMP1R2 was evaluated by monitoring the fluorescence anisotropy of DPH and TMA-DPH, as shown in Figure 9.

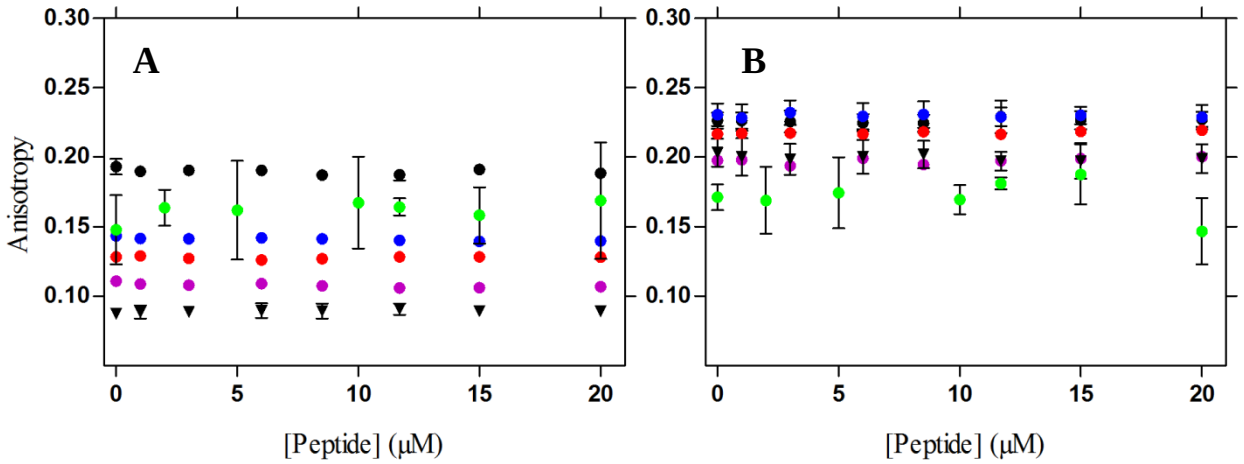

Figure 9. DPH (A) and TMA-DPH (B) fluorescence anisotropy as a function of *Ec*AMP1R2 concentration for POPC (●), POPC:POPG (70/30) (▼), POPC:Chol (70/30) (●), IML (●), OML (●) and *E. coli* cells (●). Lipid concentration was kept constant (3 mM), probe concentration was 9.9 μM and cell density 1×10^5 cells/mL.

Attending to the DPH anisotropy, in the absence of peptide, vesicles of POPC:POPG (70/30) showed the lower anisotropy values, followed by pure POPC vesicles. Lower anisotropy values are associated to a smaller restriction of rotation of the probe and, as a consequence, they correspond to membranes with higher fluidity. Thus, the most rigid LUVs were POPC:Chol (70/30), followed by *E. coli* cells and OML vesicles.

The anisotropy of TMA-DPH showed a similar pattern, with OML, POPC:Chol (70/30) and IML being the most rigid vesicles. These results are consistent with what was observed using Laurdan generalized polarization, given the close relationship between membrane fluidity and packing. Apparently, LUVs containing cholesterol or POPE are more packed and rigid, whereas increasing concentrations of CL are associated to higher fluidity and lower packing. Anisotropy results obtained for *E. coli* were close to 0.16 for DPH and 0.17 for TMA-DPH; but, once again, high standard deviations were associated to cell experiments. As to the effect of the peptide in fluidity, it did not exert significant changes neither in vesicles nor in bacterial cells, at least at the experimental conditions tested.

4.3 Changes in dipole potential

Di-8-ANEPPS was used to evaluate the effect of *Ec*AMP1R2 in the dipole potential of vesicles with different lipid compositions and *E. coli* cells. In order to quantify the interaction, we measured the ratio R for a range of peptide concentrations, as shown in Figure 10. This

ratio allows a quantitative analysis of the relative variation in dipole potential[58]. Moreover, from these results, it is possible to determinate the dissociation constant (K_d) by fitting the values to the equation 6.8. In this case, K_d is an apparent dissociation constant that describes the affinity of the peptide towards the membrane. Thus, larger values of K_d are interpreted as lower interactions. K_d values for the different vesicles tested and in *E. coli* cells are detailed in Table 4, as well as the values of ΔR, which is defined as the difference between R_0 (R in the absence of peptide) and R_{min} (i.e. the asymptotic minimum value of R).

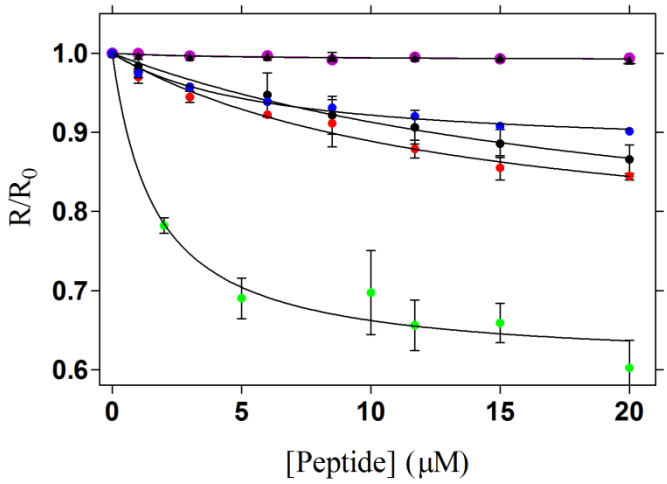

Figure 10. Dipole potential variation as a function of *Ec*AMP1R2 concentration in POPC (●), POPC:POPG (70/30) (●), POPC:Chol (70/30) (▲), IML (●), OML (●) and *E. coli* cells(●). Lipid concentration was kept constant (200 μM) and *E. coli* cells were tested at 1×10^5 cells/mL. Depicted lines represent the adjustment of the experimental data to Equation 6.8. Fitted parameters are summarized in Table 4.

Table 4: Peptide dissociation parameters by means of di-8-ANEPPS depolarization.

Lipid composition	K_d ± S.E. (μM)	ΔR
POPC	5.91 ± 5.23	-0.01
POPC:POPG (70/30)	15.18 ± 2.64	-0.23
POPC:Chol (70/30)	4.51 ± 3.13	-0.01
IML	13.38 ± 3.70	-0.26
OML	5.89 ± 1.03	-0.12
E. coli	1.66 ± 0.49	-0.39

An analysis of Figure 10 suggests that there is no change in the dipole potential of zwitterionic vesicles (*i.e.* pure POPC and POPC:Chol (70/30)). This idea is supported by the

close to zero values of ΔR (Table 4). Even with the relatively low K_d values obtained through the fitting, these should be rejected due to the high error associated to these vesicles. In contrast, *Ec*AMP1R2 induced depolarization of the OML, IML and POPC:POPG (70/30) vesicles, with K_d values of 5.89, 13.38 and 15.18 µM, respectively. The depolarization caused by *Ec*AMP1R2 in OML vesicles suggests a strong interaction, when compared to IML and POPC:POPG (70/30) vesicles. These last two show similar K_d values, implying that the peptide modifies similarly their dipole potential, and thus, that the extent to which the peptide interacts with them is alike. Interestingly, the greatest change in the membrane dipole potential induced by *Ec*AMP1R2 was observed in *E. coli* cells (K_d = 1.66 µM). We can consider that the extent to which the peptide interacts with membrane is comparable to the extent to which the peptide disturbs its dipole potential[58]. The rationale behind that is that the interaction between the peptide and membrane causes a distortion in its dipole potential, enabling to infer the affinity and strength of interaction of the peptide with *E. coli* cells, comparing the results obtained with cell membranes to those obtained with LUVs. In our case, the dissociation constant of the peptide to the cell membranes was 9 fold lower than for POPC:POPG (70/30) vesicles, having then a higher affinity for *E. coli*. Conversely, the much lower difference between OML and *E. coli*, suggests a big contribution of LPS in the interaction between peptide and membranes. Comparing these to the IML vesicles, it is LPS what mainly differentiates OML from IML.

These results can also be used to validate the results obtained in the partition studies. It confirms that *Ec*AMP1R2 selectively interacts with anionic vesicles, while the interactions with zwitterionic compositions are weak or negligible, in good agreement to the quenching assays. The big differences found between the results in *E. coli* cells and vesicles could mislead us to consider unreliable the data yielded with the chosen model membrane systems. However, it has to be taken into account that the results obtained with LUVs are representative of the interactions that happen between peptide and the lipids present in membranes. Still, bacteria cell membranes have a higher complexity, with diverse membrane proteins and other molecules that may improve the initial electrostatic interaction, hence translating into bigger differences in the dipole potential.

Overall, the membrane probes has corroborated that *Ec*AMP1R2 has a selectivity towards bacterial-like anionic membranes, as it can be inferred by the fact that only these membranes have significant changes in the different properties studied. In some cases, the interaction of

the peptide with the membranes causes a slight increase in membrane packing, but no changes in lipid fluidity have been observed. This probably could imply an internalization of the peptide into the hydrophobic core. This possibility is in good agreement with what was observed in collisional quenching studies. A deep internalization could competitively displace water molecules to the outside bulk (leading to an increase in Laurdan's G_P), without interfering in the fluidity of the membrane. Nonetheless, this is just a hypothesis and more experiences are needed to support these findings.

5. Zeta-potential of vesicles and *E. coli* in the presence of *Ec*AMP1R2

Initial interactions between AMPs and membranes (namely adsorption) are driven by electrostatic forces. Zeta-potential determination can be used to evaluate and validate the contribution of electrostatic forces to these interactions[71,72]. In this study, being *Ec*AMP1R2 a cationic peptide, it is of major importance to analyze the differences induced in the surface charge of the membrane systems. Thus, we performed zeta-potential measurements using vesicles suspensions and *E. coli* cells, in the absence and presence of *Ec*AMP1R2 (Figure 11).

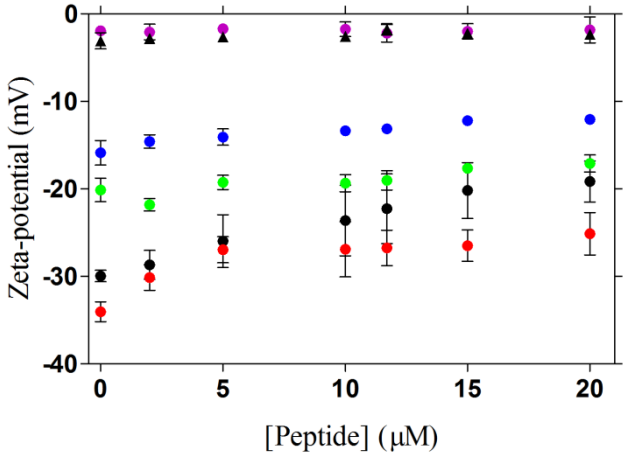

Figure 11. Zeta-potential variation as a function of *Ec*AMP1R2 concentration for POPC (●), POPC:POPG (70/30) (●), POPC:Chol (70/30) (▲), IML (●), OML (●) and *E. coli* (●). Lipid concentration was kept constant at 200 μM and *E. coli* at 1×10^5 cells/mL.

In the absence of peptide, IML vesicles displayed the highest (in absolute value) zeta-potential (ζ_0) value (-34.05 ± 1.12), followed by POPC:POPG (70/30) (ζ_0 = -29.26 ± 0.65 mV) and OML vesicles (ζ_0 = -15.88 ± 1.41 mV). On the other hand, zwitterionic vesicles [pure POPC and POPC:Chol (70/30)] showed values close to 0, as expected, as lipids that make up

these vesicles are all zwitterionic. Interestingly, the titration with *Ec*AMP1R2 did not provoke changes in the zeta-potential, indicating no interaction with these vesicles. This result is in accordance with those found in previous assays. Further addition of peptide caused a slight depolarization in OML vesicles, recording at the maximum peptide concentration (20 μM) a zeta-potential (ζ_{20}) of -12.07 ± 0.003 mV. In turn, IML vesicles showed a zeta-potential response of two phases after *Ec*AMP1R2 addition. Low concentrations of EcAMP1R2 (5 μM) caused a noticeable depolarization response. However, from this concentration on, the alteration in the zeta-potential reaches a response plateau that is maintained in the range of concentrations studied. In the case of POPC:POPG (70/30) vesicles, change in the surface charge due to increasing concentrations of added *Ec*AMP1R2 followed a linear response, but did not reach a complete neutralization in the range of concentrations studied.

In the absence of peptide, *E. coli* cells displayed a zeta-potential of -20.13 ± 1.33 mV. The addition of increasing concentrations of *Ec*AMP1R2 caused a slight neutralization on the membrane surface charge, with a behavior similar to OML vesicles. In addition, the K_d values obtained for OML and *E. coli* cells in the di-8-ANEPPS assays were also similar to those from the other vesicles. This behavior suggests a major role of LPS in peptide-bacteria affinity.

The analysis of the zeta-potential results allows us to infer some additional valuable information. Interestingly, *Ec*AMP1R2 concentrations above the MIC (11.7 μM) do not neutralize completely *E. coli* cells. This could mean two things: either the peptide reaches somehow the periplasmic space, acting thereafter in the inner membrane, or it internalizes deeply in the outer membrane, causing little surface neutralization. The peptide has shown more affinity towards the IML vesicles in the partition and quenching experiences, which could lead to think that the peptide surpasses the cell wall, acting at the inner membrane. Still, the question would be how does the peptide reach the periplasm. On the other hand, some other facts support the idea of a profound penetration into the outer membrane. Firstly, the zeta-potential behavior of OML vesicles and *E. coli* cells is very similar, and *Ec*AMP1R2 has shown to interact with model membranes mimicking the outer membrane. The integrity of the outer membrane is essential, and its disruption would irretrievably lead to cell death. However, the argument of the internalization has also a counteract. Such internalization presumably would have consequences in the lipid fluidity or packing of the membranes, and these properties remained unaffected in OML membranes.

In the case of the POPC:POPG (70/30) mixture, if we assume that the linear behavior of charge carries on, the expected concentration of peptide in which neutralization of the vesicles is achieved would be 50 µM. Manzini *et al.*[73] developed a work with an AMP with a net charge of +5 (such as *Ec*AMP1R2). In that work, they reported a neutralization of POPC:POPG (70/30) vesicles at a peptide-to-lipid ratio of 0.1. In contrast, assuming linearity in the zeta-potential of *Ec*AMP1R2 in the presence of POPC:POPG (70/30), depolarization would happen at peptide to lipid ratio of 0.25. Thus, these differences might give some force to the hypothesis of peptide internalization.

6. Studies of vesicle aggregation induced by *Ec*AMP1R2

The action of AMPs can promote aggregation of charged vesicles, usually associated with an electroneutralization of surface charge that leads to a decrease of colloidal stability[62,74]. Therefore, in the absence of peptide, no aggregation is expected, since the negative charges of the lipid headgroups would repeal each other. On the other hand, the presence of cationic peptides allows short-range interactions between the lipid membranes[75]. The ability of *Ec*AMP1R2 to induce vesicle aggregation was studied using dynamic light scattering (DLS). Variations in vesicle size are summarized in Figure 12.

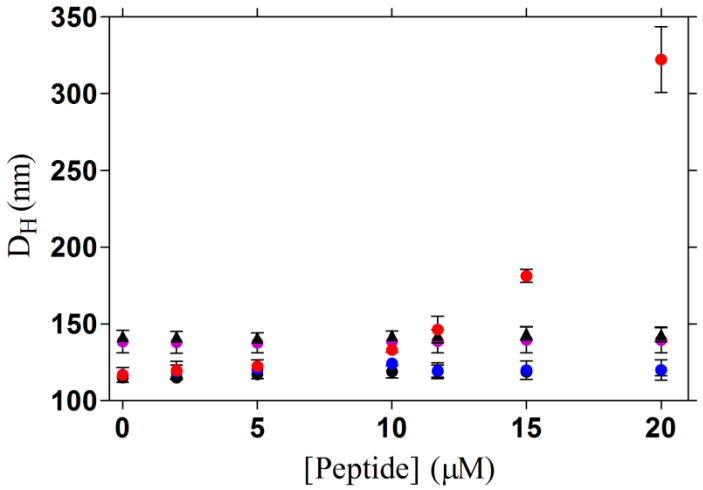

Figure 12. Alterations in the hydrodynamic diameter as a function of *Ec*AMP1R2 concentration for POPC (●), POPC:POPG (70/30) (●), POPC:Chol (70/30) (▲), IML (●), OML (●). Lipid concentration was kept constant at 200 µM.

In all cases, the size of the vesicles in the absence of peptide showed a low polydispersity. The average hydrodynamic diameter for POPC:POPG (70/30), OML and IML vesicles was

approximately 115 nm, while pure POPC and POPC:Chol (70/30) vesicles had an average size close to 140 nm.

Interestingly, *Ec*AMP1R2 only induces aggregation in IML vesicles. Aggregation of these LUVs is far of being concomitant with an electroneutralization of the vesicles (See Figure 11). The first aggregating concentration observed was 5 µM (peptide-to-lipid ratio = 0.025). From this concentration on, the extent of aggregation seems to be dose-dependent, with an increase in sample polydispersity. This threshold concentration overlaps with the range of peptide concentrations at which surface charge stabilization occurs.

When analyzing the lipid composition of the different vesicles used (Table 1), it seems that the higher content in cardiolipin is the differential trait of IML that could explain its AMP-driven aggregation tendency. POPE and POPG, the other major components of IML vesicles are also present in the OML and POPC:POPG (70/30) vesicles, but none of these aggregate. Besides, although OML vesicles also have CL, the content of this lipid is very low (1%), and previous results suggest that *Ec*AMP1R2 has an increased affinity towards LPS, thus competing with a low amount of CL molecules. We therefore hypothesize that the aggregation of IML vesicles might be due to an increased relative affinity of the peptide towards CL.

CL is an anionic phospholipid, with a small head group relative to the volume occupied by its four acyl tails. Therefore, CL is often represented with a conic geometry and has a large intrinsic negative curvature[76]. Phospholipids with intrinsic negative curvatures — not only CL, but also POPE — can self assembly into monolayers that bend back towards the headgroups, *i.e.*, with a concave shape of their hydrophilic surfaces[64]. This is the main reason why, in rod-shaped cells such as *E. coli*, CL concentrate at the membrane poles, forming finite domains[64]. Moreover, the intrinsic negative curvature of CL determine the influence of this phospholipid over the membrane environment, in terms of physical properties, increasing membrane fluidity and decreasing its packing[70]. In vesicles, it has been suggested that the morphologic features of CL can lead to local invaginations, and inter-bilayer contacts[77]. In the context of peptides and proteins, it has been extensively reported that positively charged amino-acid residues can interact with CL, reducing the electrostatic repulsion, thereby promoting the formation of CL domains[26,75,78]. The formation of such microdomains by means of the peptide has even lead to the proposal of an alternative model of AMP action, the so called *peptide-induced lipid segregation model*[79].

Thus, for the issue of how *Ec*AMP1R2 promotes IML vesicles aggregation without neutralizing their charge, we propose a hemi-fusion (or fusion) mechanism, due to a peptide-driven clustering of CL molecules. First, polycationic molecules of *Ec*AMP1R2 would gather CL molecules through electrostatic forces, forming CL microdomains. We hypothesize that the depolarization of IML vesicles at low peptide concentrations (see Figure 10) could be due to this selectivity of *Ec*AMP1R2 to the CL headgroups. The "plateau phase", in which the surface potential remains unaltered, would correspond to a stabilization of the system. In this phase, the polar headgroups of POPG would be the main contributors to the surface charge.

Thereafter, further interactions between *Ec*AMP1R2 and IML vesicles would promote a curvature deformation in the CL domains. Distortions in membrane curvatures are often caused by membrane active peptides (AMPs, FPs, CPPs and cell penetrating peptides)[13], especially in membranes rich in lipids with intrinsic negative curvature, such as POPE or CL (both present in IML vesicles)[80]. Finally, the warped outer leaflets of adjacent IML vesicles would form a concave stalk that would fuse or hemi-fuse (Figure 13), a mechanism first described by Chernomordik *et al.*[81]. This hypothesis is in good agreement with previous findings from our group[49]. In that work, it was shown, using AFM, that the leakage effect produced by $rPBI_{21}$ (an AMP) on *E. coli* cells was polar-biased. In rod shaped bacteria, these polar regions are where CL preferentially locates, due to the conic shape of this phospholipid.

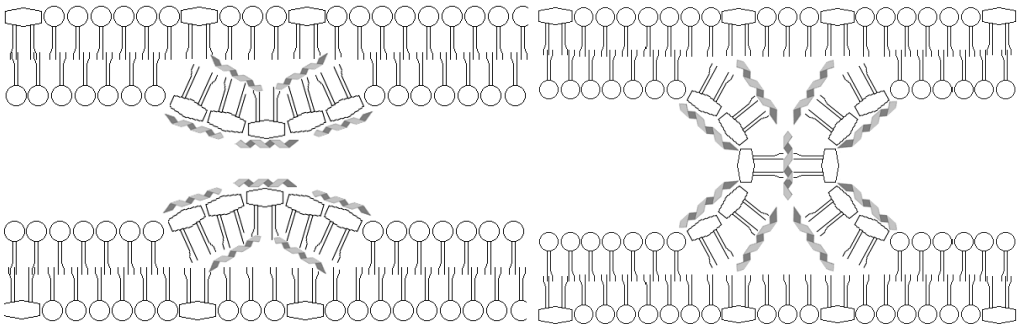

Figure 13. Scheme of the proposed peptide-driven (hemi-)fusion mechanism of IML vesicles caused by *Ec*AMP1R2. (A) Peptide-driven formation of CL (depicted as four-tailed phospholipids) microdomains. (B) Formation of concave phases and hemi-fusion. The position of the peptide in the lipid bilayer is merely illustrative.

In principle, some changes in the fluidity and packing of the vesicles would be expected when fusion or hemi-fusion takes place. However, due to the fact that IML vesicles present low amounts of CL (4 %), the clustering effect of the peptide would translate into small isolated

domains prone to (hemi-)fusion. Therefore, the peptide would favor the formation of local dynamic hemi-fusion hotspots in vesicles, increasing their hydrodynamic diameter, but that presumably would not alter the zeta-potential of the vesicles.

Altogether, our results in IML LUVs suggest an important role of the peptide-CL interaction in the destabilization of these vesicles. The confirmation of this hypothesis would imply important biological consequences. CL is an essential component of energy transducing membranes, serving as a proton trap for a subsequent proton translocation required for the ATP synthesis[64]. Besides, CL intimately interacts with many membrane proteins, including respiratory chain complexes and substrate carrier proteins[82]. Thus, given the essential role of CL domains in keeping the stability of energy transducing proteins, antimicrobial peptides might be exerting an indirect effect on the energy homeostasis of cells[83].

Besides, as the proportion of anionic lipids is relatively lower in Gram-negative bacteria than in Gram-positive bacteria, the increased affinity of *Ec*AMP1R2 towards these lipids would mean a lower peptide-to-lipid ratio necessary for the peptide to segregate anionic lipids[26]. This could explain the lower MIC value of *Ec*AMP1R2 in *E. coli*, in comparison to Gram-positive bacteria.

Conclusions and perspectives

Specific components of membranes (lipids, proteins, ions, etc.) can play a determinant role in the mode of action of AMPs. Although AMPs selectivity is sometimes seen as a merely electrostatic driven event, accumulating data[27,28,51] indicate that things are not that simple. In this work, we have investigated the selectivity and activity of *Ec*AMP1R2, a cationic AMP highly effective against *E. coli* cells. To do so, we tested lipid vesicles with increasing complexity, trying to elucidate the relative contribution of the diverse lipids to the peptide-membrane interactions. Studies with *E. coli* cells have also been performed, trying to guarantee the biological relevance of this research. We conclude that, indeed, lipid composition plays an important role in the mode of action of *Ec*AMP1R2. This AMP has a negligible affinity towards zwitterionic vesicles, as evidenced by the quenching assay and by the fact that the peptide addition does not alter any of the studied membrane physical properties. Conversely, *Ec*AMP1R2 interacts with anionic membranes, and the extent of the interaction seems to be greater for the vesicles that mimic outer and inner membranes of *E. coli* cells. Zeta-potential and di-8-ANEPPS assays results aim to a similar behavior between *E. coli* cells and outer membrane mimicking vesicles, suggesting that activity is exerted at the outer membrane level. However, *Ec*AMP1R2 seems to partition more into IML vesicles mimicking the inner membrane of *E. coli*, and increasing the lipid packing of these vesicles. However, the exact target of the peptide is still unclear and this question should be tackled. Besides, *Ec*AMP1R2 promoted vesicle aggregation of IML. Interestingly, the aggregation is not concomitant with an expected vesicle electroneutralization, which led us to propose a fusion or hemi-fusion mechanism, dependent upon the clustering of CL molecules. Briefly, *Ec*AMP1R2 would cause a lateral displacement of the CL molecules of the vesicle, creating microdomains. Thereafter, further interactions between the peptide and the CL microdomains would favor phase transition, which would result into a curvature distortion, prone to hemi-fusion. However, this hypothesis must be further addressed in future experiments. All in all, the results of this work aim to that the rationally designed peptide *Ec*AMP1R2 is a good candidate to fight Gram-negative bacteria, acting at the outer membrane level, but having also demonstrated activity in inner membrane models. An interesting possibility to explore is the ability of this peptide to act synergistically when combined with other antibiotic substances. From a therapeutic point of view, such synergistic interactions can mend some of the drawbacks associated to AMPs high costs, insufficient potency, and undesired cytotoxicity,

by allowing to reduce the dose necessary. The results of this work also highlight the importance of working with realistic model membranes, yielding valuable information that would be missed using the more simplistic models.

References

1. World Health Organization. Antimicrobial resistance. *Bull. World Health Organ.* **61,** 383–94 (2014).
2. Neill, J. I. M. O. Tackling drug-resistant infections globally: final report and recommendations. The review on antimicrobial resistance. *Rev. Antimicrob. Resist.* (2016).
3. Payne, D. J., Gwynn, M. N., Holmes, D. J. & Pompliano, D. L. Drugs for bad bugs: confronting the challenges of antibacterial discovery. *Nat. Rev. Drug Discov.* **6,** 29–40 (2007).
4. Wang, Z. & Wang, G. Antimicrobial peptide database. *Nucleic Acids Res.* **32,** D-590-D592 (2004).
5. Parham, P. *The Immune System*. (Garland Science, 2015). doi:10.1086/683765
6. Jenssen, H., Hamill, P. & Hancock, R. E. W. Peptide antimicrobial agents. *Clin. Microbiol. Rev.* **19,** 491–511 (2006).
7. Hancock, R. E. W., Haney, E. F. & Gill, E. E. The immunology of host defence peptides: beyond antimicrobial activity. *Nat. Rev. Immunol.* **16,** 321–334 (2016).
8. Veldhuizen, E. J. A., Schneider, V. A. F., Agustiandari, H., Van Dijk, A., Tjeerdsma-van Bokhoven, J. L. M., Bikker, F. & Haagsman, H.P. Antimicrobial and immunomodulatory activities of PR-39 derived peptides. *PLoS One* **9,** 1–7 (2014).
9. Gaspar, D. D., Veiga, A. S. & Castanho, M. A. R. B. From antimicrobial to anticancer peptides. A review. *Front. Microbiol.* **4,** 1–16 (2013).
10. Silva, P. M., Gonçalves, S. & Santos, N. C. Defensins: Antifungal lessons from eukaryotes. *Frontiers in Microbiology* **5,** 1–17 (2014).
11. Kaiser, E. T. & Kézdy, F. J. Secondary structures of proteins and peptides in amphiphilic environments. (A review). *Proc. Natl. Acad. Sci. U. S. A.* **80,** 1137–43 (1983).
12. Teixeira, V., Feio, M. J. & Bastos, M. Role of lipids in the interaction of antimicrobial peptides with membranes. *Progress in Lipid Research* **51,** 149–177 (2012).
13. Haney, E. F., Nathoo, S., Vogel, H. J. & Prenner, E. J. Induction of non-lamellar lipid phases by antimicrobial peptides: a potential link to mode of action. *Chem.*

Phys. Lipids **163,** 82–93 (2010).

14. Thévenet, P., Rey, J., Moroy, G., Tuffery, P., Kuczera, K., Wang, G., Ping Eng, L., Shen, T., Edwards, R., Gupta, S., Scognamiglio, P., Maccari, G., Duffy, F., Jayakanthan, M., Söllner, J., & Rhinehardt, K. *Computational peptidology*. (Springer Verlag, Hatfield, UK, 2015). doi:10.1007/978-1-4939-2285-7
15. Lee, J. & Lee, D. G. Antimicrobial peptides (AMPs) with dual mechanisms: Membrane disruption and apoptosis. *J. Microbiol. Biotechnol.* **25,** 759–764 (2014).
16. Hancock, R. E. W. & Sahl, H. G. Antimicrobial and host-defense peptides as new anti-infective therapeutic strategies. *Nat. Biotechnol.* **24,** 1551–7 (2006).
17. Melo, M. N. & Castanho, M. A. R. B. The mechanism of action of antimicrobial peptides: Lipid vesicles vs. bacteria. *Front. Immunol.* **3,** 1–4 (2012).
18. Perron, G. G., Zasloff, M. & Bell, G. Experimental evolution of resistance to an antimicrobial peptide. *Proc. R. Soc. London B* **273,** 251–256 (2006).
19. Lakshmaiah Narayana, J. & Chen, J. Y. Antimicrobial peptides: Possible anti-infective agents. *Peptides* **72,** 88–94 (2015).
20. Maria-Neto, S., de Almeida, K. C., Macedo, M. L. R. & Franco, O. L. Understanding bacterial resistance to antimicrobial peptides: from the surface to deep inside. *Biochim. Biophys. Acta* **1848,** 3078–3088 (2015).
21. Rodríguez-Rojas, A., Makarova, O. & Rolff, J. Antimicrobials, Stress and Mutagenesis. *PLoS Pathog.* **10,** (2014).
22. Wieprecht, T., Apostolov, O., Beyermann, M. & Seelig, J. Thermodynamics of the alpha-helix-coil transition of amphipathic peptides in a membrane environment: implications for the peptide-membrane binding equilibrium. *J. Mol. Biol.* **294,** 785–94 (1999).
23. Malmsten, M. Antimicrobial peptides. *Ups. J. Med. Sci.* **119,** 199–204 (2014).
24. Melo, M. N., Ferre, R. & Castanho, M. A. R. B. Antimicrobial peptides: linking partition, activity and high membrane-bound concentrations. *Nat. Rev. Microbiol.* **7,** 245–250 (2009).
25. Yeaman, M. R. & Yount, N. Y. Mechanisms of antimicrobial peptide action and resistance. *Pharmacol. Rev.* **55,** 27–55 (2003).
26. Epand, R. M. & Epand, R. F. Lipid domains in bacterial membranes and the action of antimicrobial agents. *Biochim. Biophys. Acta - Biomembr.* **1788,** 289–

294 (2009).

27. Gonçalves, S., Abade, J., Teixeira, A. & Santos, N. C. Lipid composition is a determinant for human defensin HNP1 selectivity. *Biopolymers* **98,** 313–21 (2012).
28. Gonçalves, S., Teixeira, J.,Abade, J., De Medeiros, L. N., Kurtenbach, E., & Santos, N. C. Evaluation of the membrane lipid selectivity of the pea defensin Psd1. *Biochim. Biophys. Acta - Biomembr.* **1818,** 1420–1426 (2012).
29. Brender, J. R., McHenry, A. J. & Ramamoorthy, A. Does cholesterol play a role in the bacterial selectivity of antimicrobial peptides? *Front. Immunol.* **3,** 1–4 (2012).
30. Zasloff, M. Antimicrobial peptides of multicellular organisms. *Nature* **415,** 389–395 (2002).
31. Strandberg, E., Tiltak, D., Ehni, S., Wadhwani, P. & Ulrich, A. S. Lipid shape is a key factor for membrane interactions of amphipathic helical peptides. *Biochim. Biophys. Acta - Biomembr.* **1818,** 1764–1776 (2012).
32. Schwechheimer, C. & Kuehn, M. J. Outer-membrane vesicles from Gram-negative bacteria: biogenesis and functions. *Nat. Rev. Microbiol.* **13,** 605–19 (2015).
33. Warschawski, D. E., Arnold, A. A., Beaugrand, M., Gravel, A., Chartrand, É. & Marcotte, I Choosing membrane mimetics for NMR structural studies of transmembrane proteins. *Biochimica et Biophysica Acta - Biomembranes* **1808,** 1957–1974 (2011).
34. Hancock, R. E. W. & Chapple, D. S. Peptide Antibiotics. *Antimicrob. Agents Chemother.* **43,** 1317–1323 (1999).
35. Basic structures of Prokaryotic Cells. at <https://www.boundless.com/biology/textbooks/boundless-biology-textbook/prokaryotes-bacteria-and-archaea-22/structure-of-prokaryotes-141/basic-structures-of-prokaryotic-cells-562-11775/>Date accessed: 2016-09-20
36. Pinto, J. da C., Cova, M., Ferreira, R. & Vitorino, R. Antimicrobial peptides: an alternative for innovative medicines? *Appl. Microbiol. Biotechnol.* **99,** 2023–2040 (2015).

37. Giuliani, A,. Pirri, G., Bozzi, A., Di Giulio, A., Aschi, M. & Rinaldi, A. C. Antimicrobial peptides: Natural templates for synthetic membrane-active compounds. *Cellular and Molecular Life Sciences* **65,** 2450–2460 (2008).
38. Wang, G., Xia Li & Michael Zasloff. *Antimicrobial peptides: discovery, design and novel therapeutic strategies*. (CAB International, Omaha, NE, USA, 2010). doi:10.1079/9781845936570.0000
39. Fjell, C. D., Hiss, J. A., Hancock, R. E. W. & Schneider, G. Designing antimicrobial peptides: form follows function. *Nat. Rev. Drug Discov.* **11,** 37–51 (2012).
40. Findlay, B., Zhanel, G. G. & Schweizer, F. Cationic amphiphiles, a new generation of antimicrobials inspired by the natural antimicrobial peptide scaffold. *Antimicrob. Agents Chemother.* **54,** 4049–4058 (2010).
41. Ong, Z. Y., Wiradharma, N. & Yang, Y. Y. Strategies employed in the design and optimization of synthetic antimicrobial peptide amphiphiles with enhanced therapeutic potentials. *Advanced Drug Delivery Reviews* **78,** 28–45 (2014).
42. Lakowicz, J. R. *Principles of fluorescence spectroscopy*. (Springer, New York, NY, 2006). doi:10.1007/978-0-387-46312-4
43. Santos, N. C., Prieto, M. & Castanho, M. A. R. B. Quantifying molecular partition into model systems of biomembranes: An emphasis on optical spectroscopic methods. *Biochimica et Biophysica Acta - Biomembranes* **1612,** 123–135 (2003).
44. Loura, L. M. S., De Almeida, R. F. M., Coutinho, A. & Prieto, M. Interaction of peptides with binary phospholipid membranes: Application of fluorescence methodologies. in *Chemistry and Physics of Lipids* **122,** 77–96 (2003).
45. Deslouches, B., Phadke, S. M., Lazarevic, V., Cascio, M., Montelaro, R.C. & Mietzner, T. De Novo Generation of Cationic Antimicrobial Peptides : Influence of Length and Tryptophan Substitution on Antimicrobial Activity. *Antimicrob. Agents Chemother.* **49,** 316–322 (2005).
46. Morrill, H. J., Pogue, J. M., Kaye, K. S. & LaPlante, K. L. Treatment Options for Carbapenem-Resistant Enterobacteriaceae Infections. *Ofid* 1–15 (2015). doi:10.1093/o
47. Voulgari, E., Poulou, A., Koumaki, V. & Tsakris, A. Carbapenemase-producing Enterobacteriaceae: now that the storm is finally here, how will timely detection

help us fight back? *Future Microbiol.* **8,** 27–39 (2013).

48. Mayer, L. D., Hope, M. J. & Cullis, P. R. Vesicles of variable sizes produced by a rapid extrusion procedure. *Biochim. Biophys. Acta - Biomembr.* **858,** 161–168 (1986).
49. Domingues, M. M. Silva, P. M., Franquelim, H. G., Carvalho, F. A., Castanho, M. A. R. B. & Santos, N. C. Antimicrobial protein rBPI21-induced surface changes on Gram-negative and Gram-positive bacteria. *Nanomedicine NBM* **10,** 543–551 (2014).
50. *Molecular Probes Handbook.* (Life Technologies Corporation, Carlsbad, CA, USA, 2010). doi:10.1007/978-1-61779-968-6
51. Henriques, S. T., Pattenden, L. K., Aguilar, M.-I. & Castanho, M. A. R. B. PrP(106-126) does not interact with membranes under physiological conditions. *Biophys. J.* **95,** 1877–1889 (2008).
52. Santos, N. C. & Castanho, M. A. R. B. Fluorescence spectroscopy methodologies on the study of proteins and peptides. On the 150th anniversary of protein fluorescence. *Trends Appl Spectrosc* **4,** 113–125 (2002).
53. Ladokhin, A. S., Jayasinghe, S. & White, S. H. How to measure and analyze tryptophan fluorescence in membranes properly, and why bother? *Anal. Biochem.* **285,** 235–245 (2000).
54. Melo, M. N. & Castanho, M. A. R. B. Omiganan interaction with bacterial membranes and cell wall models. Assigning a biological role to saturation. *Biochim. Biophys. Acta - Biomembr.* **1768,** 1277–1290 (2007).
55. Coutinho, A. & Prieto, M. Ribonuclease TI and Alcohol Dehydrogenase Fluorescence Quenching by Acrylamide. *J. Chem. Educ.* **70,** 1991–1994 (1993).
56. Bagatolli, L. A., Maggio, B., Aguilar, F., Sotomayor, C. P. & Fidelio, G. D. Laurdan properties in glycosphingolipid-phospholipid mixtures: A comparative fluorescence and calorimetric study. *Biochim. Biophys. Acta - Biomembr.* **1325,** 80–90 (1997).
57. Herman, P., Konopásek, I., Plásek, J. & Svobodová, J. Time-resolved polarized fluorescence studies of the temperature adaptation in Bacillus subtilis using DPH and TMA-DPH fluorescent probes. *Biochim. Biophys. Acta - Biomembr.* **1190,** 1–8 (1994).
58. Cladera, J. & O'Shea, P. Intramembrane molecular dipoles affect the membrane

insertion and folding of a model amphiphilic peptide. *Biophys. J.* **74,** 2434–42 (1998).

59. Dopico, A. *Methods in Membrane Lipids*. *ChemBioChem* (Humana Press, New York, NY, USA 2006). doi:10.1002/cbic.200800067
60. Gross, E., Bedlack, R. S. & Loew, L. M. Dual-wavelength ratiometric fluorescence measurement of the membrane dipole potential. *Biophys. J.* **67,** 208–216 (1994).
61. Wadhwani, P., Reichert, J., Bürck, J. & Ulrich, A. S. Antimicrobial and cell-penetrating peptides induce lipid vesicle fusion by folding and aggregation. *Eur. Biophys. J.* **41,** 177–187 (2012).
62. Domingues, M. M., Santiago, P. S., Castanho, M. A. R. B. & Santos, N. C. What can light scattering spectroscopy do for membrane-active peptide studies. *J. Pept. Sci.* **14,** 1084–1095 (2008).
63. Ferrão-Gonzales, A. D. Robbs, B., Moreau, V. H., Ferreira, A., Juliano, L., Silva, J. & Foguel, D Controlling B-amyloid oligomerization by the use of naphthalene sulfonates: Trapping low molecular weight oligomeric species. *J. Biol. Chem.* **280,** 34747–34754 (2005).
64. Lin, T. & Weibel, D. B. Organization and function of anionic phospholipids in bacteria. *Appl. Microbiol. Biotechnol.* **100,** 4255–4267 (2016).
65. Harris, F. M., Best, K. B. & Bell, J. D. Use of laurdan fluorescence intensity and polarization to distinguish between changes in membrane fluidity and phospholipid order. *Biochim. Biophys. Acta - Biomembr.* **1565,** 123–128 (2002).
66. Krause, M. R., Turkyilmaz, S. & Regen, S. L. Surface Occupancy Plays a Major Role in Cholesterol ' s Condensing Effect. *Langmuir* **29,** 10303–6 (2013).
67. Tanasescu, R., Lanz, M., Mueller, D., Tassler, S., Ishikawa, T., Reiter, R., Brezesinski, G. & Zumbuehl, A Vesicle Origami and the Influence of Cholesterol on Lipid Packing. *Langmuir* **32,** 4893–4903 (2016).
68. Kubiak, J., Brewer, J., Hansen, S. & Bagatolli, L. A. Lipid lateral organization on giant unilamellar vesicles containing lipopolysaccharides. *Biophys. J.* **100,** 978–986 (2011).
69. Kaiser, H. J. Surma, M., Mayer, F., Levental, I., Grzybek, M. & Lingwood, D Molecular convergence of bacterial and eukaryotic surface order. *J. Biol. Chem.* **286,** 40631–40637 (2011).

70. Unsay, J. D., Cosentino, K., Subburaj, Y. & García-Sáez, A. J. Cardiolipin effects on membrane structure and dynamics. *Langmuir* **29,** 15878–87 (2013).
71. Freire, J. M., Domingues, M., Matos, J., Melo, M., Veiga, A. S. Santos, N. C. & Castanho, M. A. R. B. Using zeta-potential measurements to quantify peptide partition to lipid membranes. *Eur. Biophys. J.* **40,** 481–487 (2011).
72. Domingues, M. M., Castanho, M. A. R. B. & Santos, N. C. rBPI21 promotes lipopolysaccharide aggregation and exerts its antimicrobial effects by (hemi)fusion of PG-containing membranes. *PLoS One* **4,** 1–8 (2009).
73. Manzini, M. C. Perez, K., Riske, K., Bozelli, J., Santos, T., Da Silva, M., Saraiva, G. K. V., Politi, M. J., Valente, A. P., Almeida, F. C. L. Chaimovich, H., Rodrigues, M., Bemquerer, M. P. Schreier, S. & Cuccovia, I. M. Peptide:Lipid ratio and membrane surface charge determine the mechanism of action of the antimicrobial peptide BP100. Conformational and functional studies. *Biochim. Biophys. Acta - Biomembr.* **1838,** 1985–1999 (2014).
74. Cametti, C. Polyion-induced aggregation of oppositely charged liposomes and charged colloidal particles: The many facets of complex formation in low-density colloidal systems. *Chem. Phys. Lipids* **155,** 63–73 (2008).
75. Beales, P. A., Bergstrom, C. L., Geerts, N., Groves, J. T. & Vanderlick, T. K. Single vesicle observations of the cardiolipin – cytochrome c interaction: induction of membrane morphology changes. *Langmuir* **4,** 6107–6115 (2011).
76. Schmidt, N. W. & Wong, G. C. L. Antimicrobial peptides and induced membrane curvature: geometry, coordination chemistry, and molecular engineering. *Curr Opin Solid State Mater Sci.* **17,** 151–163 (2013).
77. Leenhouts, J. M., de Gier, J. & de Kruijff, B. A novel property of a mitochondrial presequence. Its ability to induce cardiolipin-specific interbilayer contacts which are dissociated by a transmembrane potential. *FEBS Lett.* **327,** 172–176 (1993).
78. Epand, R. F., Tokarska-SCholattner, M., SCholattner, U., Wallimann, T. & Epand, R. M. Cardiolipin Clusters and Membrane Domain Formation Induced by Mitochondrial Proteins. *J. Mol. Biol.* **365,** 968–980 (2007).
79. Arouri, A., Dathe, M. & Blume, A. Peptide induced demixing in PG/PE lipid mixtures: A mechanism for the specificity of antimicrobial peptides towards bacterial membranes? *Biochim. Biophys. Acta - Biomembr.* **1788,** 650–659 (2009).

80. Koller, D. & Lohner, K. The role of spontaneous lipid curvature in the interaction of interfacially active peptides with membranes. *Biochim. Biophys. Acta - Biomembr.* **1838,** 2250–2259 (2014).
81. Chernomordik, L., Chanturiya, a, Green, J. & Zimmerberg, J. The hemifusion intermediate and its conversion to complete fusion: regulation by membrane composition. *Biophys. J.* **69,** 922–929 (1995).
82. Paradies, G., Paradies, V., De Benedictis, V., Ruggiero, F. M. & Petrosillo, G. Functional role of cardiolipin in mitochondrial bioenergetics. *Biochim. Biophys. Acta - Bioenerg.* **1837,** 408–417 (2014).
83. Hurdle, J. G., O'Neill, A. J., Chopra, I. & Lee, R. E. Targeting bacterial membrane function: an underexploited mechanism for treating persistent infections. *Nat. Rev. Microbiol.* **9,** 62–75 (2010).